

Direct comparison of many-body methods for realistic electronic Hamiltonians

(Simons collaboration on the many-electron problem)

Kiel T. Williams,¹ Yuan Yao,² Jia Li,³ Li Chen,¹ Hao Shi,^{4,5} Mario Motta,⁶ Chunyao Niu,^{5,7} Ushnish Ray,⁸ Sheng Guo,⁸ Robert J. Anderson,⁹ Junhao Li,² Lan Nguyen Tran,^{3,10} Chia-Nan Yeh,³ Bastien Mussard,¹¹ Sandeep Sharma,¹¹ Fabien Bruneval,¹² Mark van Schilfhaarde,⁹ George H. Booth,⁹ Garnet Kin-Lic Chan,⁸ Shiwei Zhang,^{4,5} Emanuel Gull,³ Dominika Zgid,^{3,10} Andrew Millis,^{4,13} Cyrus J. Umrigar,² and Lucas K. Wagner¹

¹*Department of Physics, University of Illinois at Urbana-Champaign*

²*Laboratory of Atomic and Solid State Physics, Cornell University, Ithaca, NY 14853*

³*Department of Physics, University of Michigan, Ann Arbor, MI 48109*

⁴*Center for Computational Quantum Physics, Flatiron Institute, New York, NY 10010*

⁵*Department of Physics, College of William and Mary, Williamsburg, VA 23185*

⁶*IBM Almaden Research Center, 650 Harry Road, San Jose, CA 95120, USA*

⁷*School of Physics and Engineering, Zhengzhou University, Zhengzhou 450001, China*

⁸*California Institute of Technology, Pasadena, CA 91125*

⁹*Department of Physics, King's College London, Strand, London, WC2R 2LS, U.K*

¹⁰*Department of Chemistry, University of Michigan, Ann Arbor, MI 48104*

¹¹*Department of Chemistry, University of Colorado, Boulder*

¹²*DEN, Service de Recherches de Métallurgie Physique, CEA, Université Paris-Saclay, F-91191 Gif-sur-Yvette, France*

¹³*Department of Physics, Columbia University, New York, NY 10027*

A large collaboration carefully benchmarks 20 first principles many-body electronic structure methods on a test set of 7 transition metal atoms, and their ions and monoxides. Good agreement is attained between 3 systematically converged methods, resulting in experiment-free reference values. These reference values are used to assess the accuracy of modern emerging and scalable approaches to the many-electron problem. The most accurate methods obtain energies indistinguishable from experimental results, with the agreement mainly limited by the experimental uncertainties. Comparison between methods enables a unique perspective on calculations of many-body systems of electrons.

INTRODUCTION

A major challenge in condensed matter physics, materials physics, and chemistry is to compute the properties of electronic systems using realistic Hamiltonians. Efficient and accurate calculations could enable computational design of drugs[1] and other materials,[2, 3] and shed light on a number of physical questions, such as the origin of linear-T resistivity,[4] high temperature superconductivity,[5] and many other effects that currently lack satisfying explanation.

Many-body quantum calculations on classical computers are challenging because the dimension of the Hilbert space increases dramatically with the number of particles. For example, in the simple case of a CuO molecule with a large (5z) basis, the Hilbert space is of dimension 10^{44} for the $S_z = \frac{1}{2}$ sector. A vector of this size cannot be represented in any computer; at the present time the Oak Ridge machine Summit has approximately 250 petabytes of storage,[6] which is still approximately 17 orders of magnitude too small to store a single vector. Modern techniques therefore use compression and other techniques to approximate the state vectors.

There are many, not always mutually exclusive, approaches to dealing with the dimensionality: truncation of the wave function space through wave function *ansatzes*, one-particle Green function approaches, den-

sity functional theory, Monte Carlo methods, and embedding techniques. The techniques vary dramatically in their computational cost and accuracy. Most studies[7–15] judge the accuracy of the methods by comparing to experimental energies,[16] which are computed by taking differences of total energies and are therefore subject to fortuitous cancellation of error. Instead, in this study we include 3 systematically improvable methods with sufficiently small prefactors that they yield almost exact total energies within the chosen basis set and serve as a benchmark for testing all other methods.

In this manuscript, we apply a diverse array of 20 established and emerging techniques to a test set of small, realistic transition metal molecules and atoms. Each technique was implemented by an expert, and employed precisely the same Hamiltonian. This approach allows us to directly assess methodological differences without confounders such as different Hamiltonians, and has been important for a previous benchmark study of the hydrogen chain.[17] For these systems, we achieve convergence of exponentially scaling but systematically convergeable methods at the order of 1 mHartree in the *total energy*, or about 300 K, establishing a reliable reference on realistic Hamiltonians with complex atoms. We then assess the accuracy of more approximate approaches for computing the total energy of atoms and molecules, which allows some assessment of transferability of performance

with increasing system size. Finally, we study how errors in the total energies translate into errors of physical observables obtained as differences of total energies, and we make comparisons to experiments. These results provide an important reference for the development of techniques that can address the larger goal of computing electronic properties of realistic materials.

METHODOLOGY

Table I lists the methods tested in this work. It includes most of the common techniques to address the many-electron problem, as well as some emerging methods. It also includes a few methods such as CISD which are no longer commonly used but have historical relevance. The methods in this benchmark vary dramatically in their computational cost; the density functional theory methods required only a few minutes to complete the test set, while some of the more advanced techniques were not able to treat every basis for every system with the available amount of computer time. The methods also scale very differently, ranging from $\mathcal{O}(N_e^3)$ to exponential in the number of electrons N_e . Of the 3 systematically converged methods (iFCIQMC, DMRG and SHCI) only SHCI was performed for all the systems in all the basis sets. Consequently, SHCI energies will be used as the reference.

Some of the other techniques are in principle systematically improvable, such as configuration interaction, coupled cluster, self-energy embedding theory, and the Monte Carlo methods, but convergence to better than 1 mHa was not achieved on these systems for the level of the method employed. Some of the techniques give upper bounds to the exact energy, such as DMC, CISD, DMRG, and HF. Finally, for completeness it should be noted that the methods also require different levels of specification to define the approximations used. For example, some of the methods can be reproduced only by specifying the initial starting determinant; others require defining an initial multideterminantal wavefunction, or the choice of partitioning between high-level and low-level methods.

We consider transition metal systems, with the core electrons removed using effective core potentials[51–53]. These potentials accurately represent the core[54] in many-body simulations and allow all the methods considered in this work to use the same Hamiltonian. In addition, they provide an easy way to include scalar relativistic effects, needed for meaningful comparison to experiment. These potentials are available for O, Sc, Ti, V, Cr, Mn, Fe, and Cu, which defines our test set. We consider these atoms, their ions, and the corresponding transition metal monoxide molecules. To simplify the comparison, the molecules were computed at their equilibrium geometry.

Almost every electronic structure method (all the

TABLE I. A list of abbreviations used in this benchmark. Details are available in the Supplementary Material. Column A lists the largest basis set employed by that method for at least one of the transition metal atoms, Column B lists the same for the monoxide molecules. The basis sets are abbreviated in order as d, t, q, 5, and c for complete basis set.

Abbreviation	Method	A	B
AFQMC(MD)	Auxiliary field quantum Monte Carlo with a multi-determinant trial function[18, 19]	5	5
B3LYP	DFT with the B3LYP functional[20]	5	5
CISD	Configuration interaction with singles and doubles	5	5
DMC(SD)	Fixed node diffusion Monte Carlo with a single determinant nodal surface[21, 22]	c	c
DMRG	Density matrix renormalization group[23, 24]	t	d
GF2	Second order Green function[25, 26]	q	q
HF	Hartree-Fock	5	5
HF+RPA	Hartree-Fock random phase approximation[27]	t	t
HSE06	DFT with the HSE06 functional[28, 29]	5	5
iFCIQMC	Initiator full configuration interaction quantum Monte Carlo[30, 31]	q	d
LDA	DFT in the local density approximation[32, 33]	5	5
MRLCC	Multireference localized coupled cluster[34–37]	5	5
PBE	DFT in the PBE[38] approximation	5	5
QSGW	Quasiparticle self-consistent GW approximation[39]	t	t
SCAN	DFT with SCAN functional[40]	5	5
SC-GW	Self-consistent GW approximation[41, 42]	t	-
SEET(FCI/GF2)	Self-energy embedding theory with many-body expansion.[43–47]	q	q
SHCI	Semistochastic heatbath configuration interaction[48, 49]	5	5
UCCSD	Unrestricted coupled cluster with singles and doubles[50]	5	5
UCCSD(T)	Unrestricted coupled cluster with singles, doubles, and perturbative triples[50]	5	5

methods in this study except DMC) works in a finite basis. Here, we follow the chemistry convention of defining an ascending basis set denoted by the $z(\zeta)$ value, ranging from 2 to 5; i.e., dz, tz, qz, and 5z. For each system, we consider the first principles Hamiltonian projected onto the basis, making for a total of $23 \times 4 = 98$ calculations for each method. See the Supplementary Material for details on the precise basis sets used in this study. While the results are only comparable to experiment in the complete basis set limit (cbs), for each basis set there corresponds a projected Hamiltonian, which also has an exact solution. We thus can compare methods *within a basis* since the Hamiltonian is defined precisely.

In Table I, we list the methods considered in this work. The deviation in the total energy between two methods m and n is computed as

$$\sigma(m, n) = \sqrt{\frac{\sum_{i \in \text{systems}} (E_i(n) - E_i(m))^2}{N}}, \quad (1)$$

where N is the total number of calculations performed

in common between the methods. This is a measure of how well the output total energies between two methods agree. It is possible for two methods with large σ to agree on energy *differences* if there is significant cancellation of errors.

To compare total energies between methods and systems in a consistent way, we use the concept of percent of correlation, commonly used in quantum chemistry:

$$\% \text{ correlation energy}(m) = 100 \times \frac{E_{\text{HF}} - E_m}{E_{\text{HF}} - E_{\text{SHCI}}}, \quad (2)$$

where E_{HF} is the Hartree-Fock energy, m stands for the method under consideration, and E_{SHCI} is the total energy computed in the basis by the SHCI method. At 100% of the correlation energy, the exact result is obtained. This quantity is particularly useful since methods tend to obtain similar percentages of the correlation energy across different basis sets and systems.

Extrapolation to the basis set limit is done making the usual assumption that the correlation energy (difference between Hartree-Fock and the exact energy) scales as $1/n^3$, where n is the cardinal number of the basis set, and that the Hartree-Fock energy exponentially converges to the complete basis limit. Complete basis set extrapolation is necessary for comparison of the finite basis set results to experiment, diffusion Monte Carlo (DMC), and density functional theory results. DMC works directly in the complete basis limit, whereas density functional methods are designed to reproduce complete basis set limit energies. The uncertainty in the extrapolation, judged from the variation between different fits to the extrapolation, is approximately 2–4 mHa; for details, see the Supplementary Material. Thus, in this test set, the largest uncertainty in the complete basis set total energy is due to the extrapolation of finite basis set energies to the infinite limit.

The energy differences studied are the ionization potential of a transition metal atom M : $\text{IP} = E(M^+) - E(M)$, and the dissociation energy of a metal oxide molecule MO : $\text{DE} = E(M) + E(O) - E(MO)$. These quantities have been studied in detail for these systems in the past, for example Refs [7–13, 55–58], among others. However, none of these previous studies have attained reference energies as well-converged as the ones in this paper, and none compare energies from a large number of methods.

RESULTS

We show several views of the data collected in this study in the figures. The Supplementary Material contains various tables and the complete set of data (~ 1200 calculations) on which these plots are based. Fig 1 establishes that several high accuracy techniques are in agreement and establishes a reference technique SHCI. Fig 2

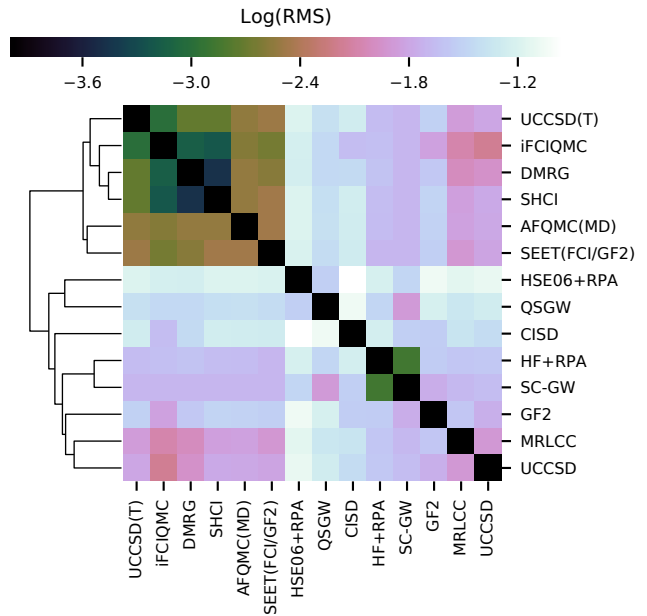


FIG. 1. Cluster analysis of electronic structure methods in this work. The matrix values are the logarithm of the RMS deviation of the total energy in Hartrees (Eq. 1) between the two methods.

compares the performance of methods in computing the total energy as compared to the reference. Fig 3 compares the performance of methods in computing ionization potential of the atoms and dissociation energy of the molecules. Fig 4 summarizes the cancellation of error for different techniques in computing the differences in energies. Finally, Fig 5 compares calculations using methods found to be accurate to the experimental dissociation energies. In this section, we examine related methods in the context of these different views.

In Fig 1, we show a cluster analysis of the total energies using Eq. 1, evaluated on the intersection of basis sets and systems available for both methods, as the distance metric. iFCIQMC, DMRG and SHCI were converged to very high levels of accuracy. In fact these three methods agree to ~ 1 mHa for all systems and basis sets that were computed. Because of this 3-fold agreement, we can take any of these results as the exact ground state energy in a given basis set to within an RMS error of less than 1 mHa, which is approximately what is termed “chemical accuracy” in the context of energy differences. Here we have achieved 1 mHa accuracy in the total energy of the ground state. However, as shown in Table I, iFCIQMC and DMRG calculations were feasible within the available computer time for only the smaller basis sets, so we use SHCI as the reference. For finite basis sets, the estimated uncertainty is ~ 1 mHa, and for the complete basis set, the estimated uncertainty is ~ 2 –4 mHa due to the extrapolation uncertainty.

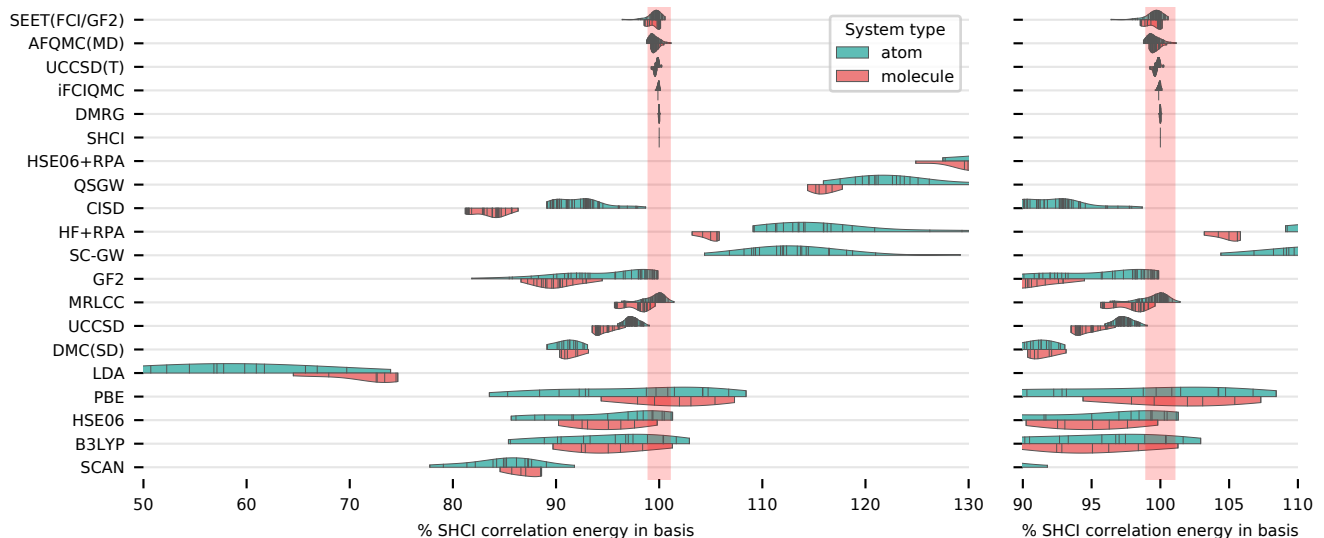


FIG. 2. Kernel density estimation[59–61] of the percent of the SHCI-computed correlation energy within each basis obtained by each of the methods in the benchmark set. All basis sets available are plotted; individual data points are indicated by small lines.

Density functional methods have a large spread across systems in the percent of correlation energy attained (Fig 2). The gradient corrected and the hybrid functionals (B3LYP, HSE06, PBE and SCAN) improve the LDA. The most recently proposed of these, SCAN, is more consistent in the percent of correlation energy obtained at around 80–90% of the correlation energy. Fig. 4 shows that it also benefits more than the other functionals from a cancellation of errors between the atom and the molecule to give more accurate dissociation energies, although it has less cancellation of errors for the ionization potentials. Much of the improvement in accuracy of the hybrid functionals over PBE is in the cancellation of error.

The random phase approximation (RPA) and both versions of GW overestimate the correlation energy as shown in Fig 2. While the total energy tends to be too low, those errors tend to cancel for QSGW applied to energy differences, as can be seen in Figs. 3 and 4.

As can be seen in Fig 2, configuration interaction with singles and doubles (CISD), a truncated determinant expansion technique well-known to have size consistency defects, performs much better for the atoms than the molecules, which leads to rather poor predictions for the dissociation energy of the molecules (Fig 3). The error is large enough that CISD was not included in Fig 4 to improve readability of the more accurate numbers. We note that unrestricted coupled cluster with singles and doubles (UCCSD), which is size consistent, also performs worse on the molecules than the atoms, though to a lesser degree than CISD. This results in underestimation of the dissociation energy (Fig 3), and no cancellation of error

in the dissociation energy, but significant cancellation in the ionization potential (Fig 4).

Fixed node diffusion Monte Carlo with a single determinant trial function (DMC(SD)) yields a lower bound to the extrapolated correlation energy, corresponding to an upper bound to the total energy, which is apparent in Fig 2. The remaining energy is the fixed node error, the main approximation in the DMC calculations, which for a single Slater determinant nodal surface is much larger than the extrapolation uncertainty. With the single Slater determinant, DMC obtains 90–95% of the correlation energy quite consistently, in line with previous benchmarks on smaller systems[62]. This consistency results in significant cancellation of error (Fig 4) in the dissociation energy and ionization potential.

Self energy embedding theory with a full configuration interaction solver and GF2 embedding (SEET(FCI/GF2)) obtains results in good agreement with the reference total energy (Fig 2), resulting in accurate energy differences (Fig 3). Consequently, it lies very close to the $x = y$ line in Fig 4 and does not benefit from additional cancellation of error, as the energies are already accurate. The errors in the total energy are not strongly correlated with the atomic species; for example the error in the Ti atom is not statistically similar to the error in the TiO atom, resulting in little cancellation of error.

The auxilliary field quantum Monte Carlo with a multiple determinant trial function (AFQMC(MD)) gives good agreement with the reference total energy, with an RMS deviations of about 3 to 4 mHa. The dissociation energies have an RMS deviation of ~ 2.5 mHa, which is

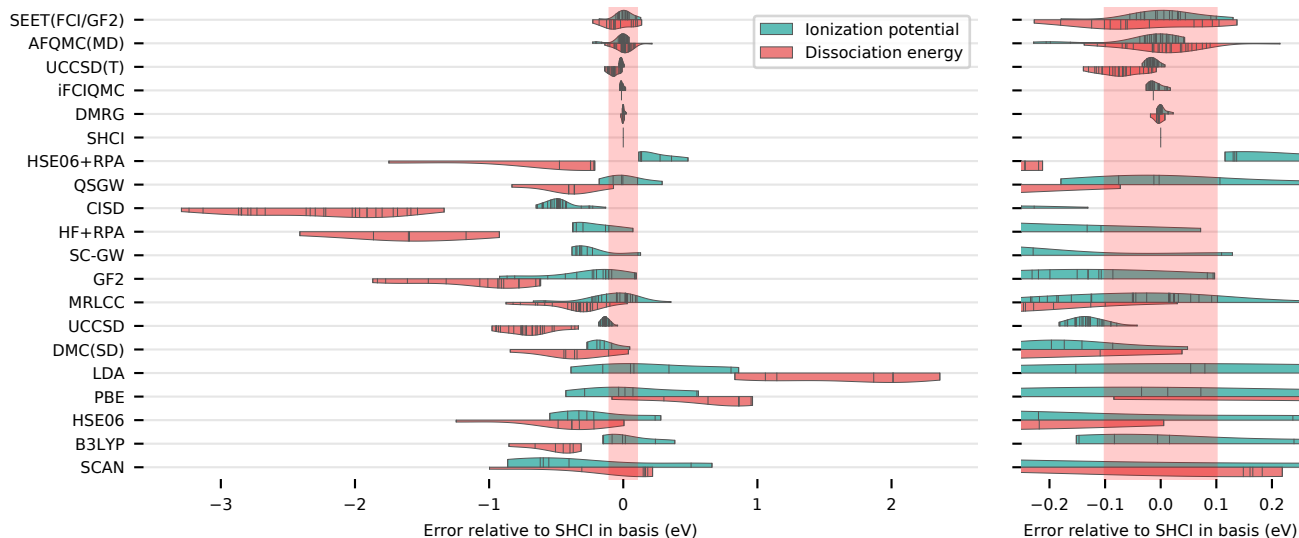


FIG. 3. Kernel density estimation plot of dissociation energy and ionization potential of molecules and atoms to SHCI reference calculations. Methods are ordered according to the clustering in Fig 1.

consistent with the conclusion of a recent benchmark on a large set of transition metal diatomics [14]. The use of single determinant UHF trial wave functions would lead to less accurate results, roughly doubling the RMS error in the total energy of the molecules (see Supplementary Material I.A).

Coupled cluster with singles, doubles, and perturbative triples (UCCSD(T)) performs very well on these systems, obtaining close to 100% of the correlation energy. For these problems, UCCSD(T) has a notably low cost for high performance. The accuracy of UCCSD(T) is likely due to the fact that these systems are not strongly multi-reference, in that even in the near-exact wave functions, there is a single dominant determinant that makes a large contribution to the wave function. This can be seen by examining the natural orbital occupations; for example in UCCSD, the spin-resolved natural orbitals with large occupations have occupations of 0.96 or greater. The single reference nature also explains the mediocre performance of the multi-reference methods such as MRLCC, which sacrifice some accuracy in the single reference case to treat multi-reference situations more accurately. In general, active space techniques, which operate within an explicitly chosen subspace of the larger Hilbert space, are not very effective for these systems.

We believe that the reference data produced computationally has lower uncertainties than experiment for the purposes of benchmarking quantum calculation techniques. The ionization potential of the large-basis SHCI results is in agreement with experiment with mean absolute deviation of 0.2 mHa, or 7 meV, so one could equivalently use experiment or the SHCI reference values, as can be verified in Table VI of the Supplementary Material.

The experimental dissociation energy estimation is limited by the challenges of the measurements and the experimental measures differ from one another by as much as 0.5 eV. In Fig 5, the high accuracy estimates of the dissociation energy of the molecules is shown, compared to experimental values with zero point energy removed [63–69]. For these systems, the experimental uncertainty of the dissociation energy is larger than the difference between the most accurate techniques in this benchmark. Remarkably, SHCI, UCCSD(T), and AFQMC(MD) agree to about 0.1 eV for all the molecules. We also should note that since we used effective core potentials to standardize the benchmark, there may be some small errors in comparing directly to experiment. However, we see no evidence that the potentials used are limiting the accuracy; the most accurate methods obtain results well within the experimental uncertainty, with the possible exception of VO, for which most of the experimental values are slightly below the theoretical ones.

When computing differences of total energies, both methodological errors and errors due to finite basis sets tend to cancel. In Fig 4 we quantify the methodological cancellation of errors in many of the techniques studied in this work. Considering basis set errors, the RMS error in the total energy in the commonly used *tz* basis compared to the complete basis set limit is 75 mHa, while the RMS error in the ionization energy and dissociation energy for the same comparison are 1.6 mHa and 6 mHa respectively, as can be seen in Table VIII in the Supplementary information.

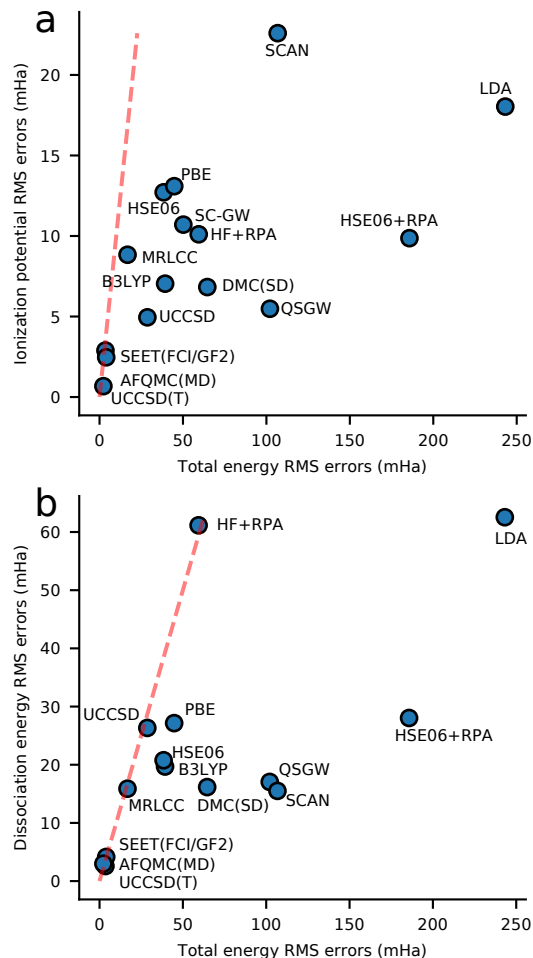


FIG. 4. Cancellation of error for many methods in this study, computed by comparing the RMS error in the total energy to the RMS error in the (a) ionization energy of the atoms and (b) dissociation energy for molecules. HF and CISD were excluded from the comparison for more detail in the more accurate methods; they are off the scale here. The red dashed line corresponds to no cancellation of error.

CONCLUSION

We surveyed 20 advanced many-electron techniques on precisely defined realistic Hamiltonians for transition metal systems. For a given basis set, we achieved ~ 1 mHa agreement on the total energy between high accuracy methods, which provides a *total energy* benchmark for many-body methods. To our knowledge, such an agreement is unprecedented for first principles calculations of transition metal systems. Our accurate reference energies should enable the development of approximate, but more computationally efficient, many-body techniques as well as better density functionals, without the necessity of experimental reference values. These systems are also a useful test for future quantum comput-

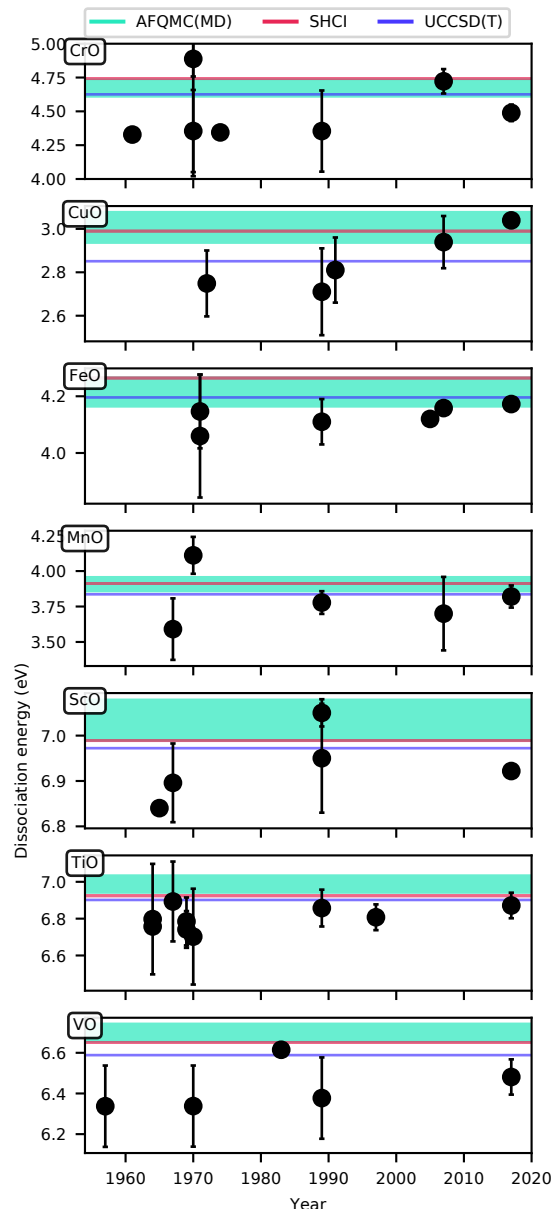


FIG. 5. Comparison of 5z dissociation energies of the transition metal molecules obtained from the more accurate methods used in this work to experiment. The x-axis is the year the experimental result was published and the width of the bars indicate statistical/systematic uncertainties.

ing algorithms. To enable such comparisons, we include `pyscf` scripts that can execute the benchmark for any density functional available in `libxc`[70], and can export the one- and two-body integrals needed for testing many-body methods.

We have assessed the state of the art in achieving high accuracy in realistic systems. The benchmark set includes systems with large Hilbert spaces of around 10^{44} determinants. While these spaces are so large that a

single vector cannot fit in any computer memory, the computations are feasible due to powerful compression of that space. The systematically converged techniques used in this work (DMRG, FCIQMC, and SHCI), were able to achieve excellent agreement, but can be applied only to relatively small systems due to their computational cost. It is thus important to understand the errors in lower-scaling techniques that can be applied to larger systems, and whether performance on small systems is transferable to larger systems. Our study takes a step in that direction, since we were able to achieve converged results for both correlated atoms and molecules, and indeed we observed that the accuracy of some techniques degrades with system size.

To avoid misinterpretation of the results, we make a comment here. In order to ensure high quality results, it was necessary to limit the number of systems on which this benchmark was performed. While treating electron correlation accurately is important to obtain accurate results, these systems have a particular character of correlation. In a determinant expansion of the wave function, the systems chosen here have one determinant with a large weight and many determinants with small weights, rather than several determinants with large weights. For such systems, methods such as UCCSD(T) are accurate. The performance profile will likely be different for differently correlated chemical systems, so benchmarking efforts of similar quality in that realm would be highly valuable.

This work was supported by a grant from the Simons Foundation as part of the Simons Collaboration on the Many Electron Problem.

-
- [1] D. C. Young, *Computational drug design: a guide for computational and medicinal chemists* (John Wiley & Sons, 2009).
- [2] Z. W. Seh, J. Kibsgaard, C. F. Dickens, I. Chorkendorff, J. K. Nørskov, and T. F. Jaramillo, *Science* **355**, eaad4998 (2017).
- [3] S. Curtarolo, G. L. W. Hart, M. B. Nardelli, N. Mingo, S. Sanvito, and O. Levy, *Nature Materials* **12**, 191 (2013).
- [4] J. a. N. Bruin, H. Sakai, R. S. Perry, and A. P. Mackenzie, *Science* **339**, 804 (2013).
- [5] K. A. Müller and J. G. Bednorz, *Science* **237**, 1133 (1987).
- [6] J. Hines, *Computing in Science Engineering* **20**, 78 (2018).
- [7] C. W. Bauschlicher and P. Maitre, *Theoretica chimica acta* **90**, 189 (1995).
- [8] F. Furche and J. P. Perdew, *The Journal of Chemical Physics* **124**, 044103 (2006).
- [9] K. Doblhoff-Dier, J. Meyer, P. E. Hoggan, G.-J. Kroes, and L. K. Wagner, *Journal of Chemical Theory and Computation* **12**, 2583 (2016).
- [10] P. Verma, Z. Varga, J. E. M. N. Klein, C. J. Cramer, L. Q. Jr, and D. G. Truhlar, *Physical Chemistry Chemical Physics* (2017), 10.1039/C7CP01263B.
- [11] X. Xu, W. Zhang, M. Tang, and D. G. Truhlar, *Journal of Chemical Theory and Computation* **11**, 2036 (2015).
- [12] Y. Minenkov, E. Chermak, and L. Cavallo, *Journal of Chemical Theory and Computation* **12**, 1542 (2016).
- [13] R. E. Thomas, G. H. Booth, and A. Alavi, *Physical Review Letters* **114**, 033001 (2015).
- [14] J. Shee, B. Rudsteyn, E. J. Arthur, S. Zhang, D. R. Reichman, and R. A. Friesner, *Journal of Chemical Theory and Computation* **15**, 2346 (2019), pMID: 30883110, <https://doi.org/10.1021/acs.jctc.9b00083>.
- [15] J. Shee, E. J. Arthur, S. Zhang, D. R. Reichman, and R. A. Friesner, *Journal of Chemical Theory and Computation* **14**, 4109 (2018).
- [16] R. H. Page and C. S. Gudeman, *JOSA B* **7**, 1761 (1990).
- [17] M. Motta, D. M. Ceperley, G. K.-L. Chan, J. A. Gomez, E. Gull, S. Guo, C. A. Jiménez-Hoyos, T. N. Lan, J. Li, F. Ma, A. J. Millis, N. V. Prokof'ev, U. Ray, G. E. Scuseria, S. Sorella, E. M. Stoudenmire, Q. Sun, I. S. Tupitsyn, S. R. White, D. Zgid, and S. Zhang (Simons Collaboration on the Many-Electron Problem), *Phys. Rev. X* **7**, 031059 (2017).
- [18] S. Zhang and H. Krakauer, *Phys. Rev. Lett.* **90**, 136401 (2003).
- [19] M. Motta and S. Zhang, *Wiley Interdisciplinary Reviews: Computational Molecular Science* **8**, e1364 (2018), <https://onlinelibrary.wiley.com/doi/pdf/10.1002/wcms.1364>.
- [20] A. D. Becke, *The Journal of Chemical Physics* **98**, 5648 (1993).
- [21] W. M. C. Foulkes, L. Mitas, R. J. Needs, and G. Rajagopal, *Reviews of Modern Physics* **73**, 33 (2001).
- [22] L. K. Wagner, M. Bajdich, and L. Mitas, *Journal of Computational Physics* **228**, 3390 (2009).
- [23] R. Olivares-Amaya, W. Hu, N. Nakatani, S. Sharma, J. Yang, and G. K.-L. Chan, *The Journal of chemical physics* **142**, 034102 (2015).
- [24] S. Sharma and G. K.-L. Chan, *The Journal of chemical physics* **136**, 124121 (2012).
- [25] J. J. Phillips and D. Zgid, *The Journal of Chemical Physics* **140**, 241101 (2014), <https://doi.org/10.1063/1.4884951>.
- [26] A. A. Rusakov and D. Zgid, *The Journal of Chemical Physics* **144**, 054106 (2016), <https://doi.org/10.1063/1.4940900>.
- [27] H. Eshuisa, J. Yarkony, and F. Furche, *J. Chem. Phys.* **132**, 234114 (2010).
- [28] J. Heyd, G. E. Scuseria, and M. Ernzerhof, *J. Chem. Phys.* **118**, 8207 (2003).
- [29] J. Heyd, G. E. Scuseria, and M. Ernzerhof, *The Journal of Chemical Physics* **124**, 219906 (2006).
- [30] G. H. Booth, A. J. W. Thom, and A. Alavi, *The Journal of Chemical Physics* **131**, 054106 (2009), <https://aip.scitation.org/doi/pdf/10.1063/1.3193710>.
- [31] D. Cleland, G. H. Booth, and A. Alavi, *The Journal of Chemical Physics* **132**, 041103 (2010), <https://doi.org/10.1063/1.3302277>.
- [32] D. M. Ceperley and B. J. Alder, *Physical Review Letters* **45**, 566 (1980).
- [33] S. H. Vosko, L. Wilk, and M. Nusair, *Canadian Journal of Physics* **58**, 1200 (1980).
- [34] S. Sharma and A. Alavi, *The Journal of Chemical Physics* **143**, 102815 (2015).
- [35] S. Sharma, G. Jeanmairet, and A. Alavi, *The Journal of*

- Chemical Physics **144**, 034103 (2016).
- [36] G. Jeanmairet, S. Sharma, and A. Alavi, The Journal of Chemical Physics **146**, 044107 (2017).
- [37] S. Sharma, G. Knizia, S. Guo, and A. Alavi, Journal of Chemical Theory and Computation **13**, 488 (2017).
- [38] J. P. Perdew, K. Burke, and M. Ernzerhof, Physical Review Letters **77**, 3865 (1996).
- [39] S. V. Faleev, M. van Schilfgaarde, and T. Kotani, Phys. Rev. Lett. **93**, 126406 (2004).
- [40] J. Sun, A. Ruzsinszky, and J. Perdew, Physical Review Letters **115**, 036402 (2015).
- [41] L. Hedin, Phys. Rev. **139**, A796 (1965).
- [42] T. N. Lan, A. Shee, J. Li, E. Gull, and D. Zgid, Phys. Rev. B **96**, 155106 (2017).
- [43] T. N. Lan, A. A. Kananenka, and D. Zgid, J. Chem. Phys. **143**, 241102 (2015), <http://dx.doi.org/10.1063/1.4938562>.
- [44] T. N. Lan and D. Zgid, The Journal of Physical Chemistry Letters **8**, 2200 (2017), pMID: 28453934, <https://doi.org/10.1021/acs.jpclett.7b00689>.
- [45] D. Zgid and E. Gull, New Journal of Physics **19**, 023047 (2017).
- [46] L. N. Tran, S. Iskakov, and D. Zgid, The Journal of Physical Chemistry Letters **9**, 4444 (2018), pMID: 30024163, <https://doi.org/10.1021/acs.jpclett.8b01754>.
- [47] A. A. Rusakov, S. Iskakov, L. N. Tran, and D. Zgid, Journal of Chemical Theory and Computation **15**, 229 (2019), <https://doi.org/10.1021/acs.jctc.8b00927>.
- [48] A. A. Holmes, N. M. Tubman, and C. J. Umrigar, J. Chem. Theory Comput. **12**, 3674 (2016).
- [49] J. Li, M. Otten, A. A. Holmes, S. Sharma, and C. J. Umrigar, J. Chem. Phys. **148**, 214110 (2018).
- [50] R. J. Bartlett and M. Musia, Reviews of Modern Physics **79**, 291 (2007).
- [51] J. R. Trail and R. J. Needs, The Journal of Chemical Physics **139**, 014101 (2013).
- [52] J. R. Trail and R. J. Needs, The Journal of Chemical Physics **142**, 064110 (2015).
- [53] J. R. Trail and R. J. Needs, The Journal of Chemical Physics **146**, 204107 (2017).
- [54] M. C. Bennett, C. A. Melton, A. Annaberdiyev, G. Wang, L. Shulenburger, and L. Mitas, The Journal of Chemical Physics **147**, 224106 (2017).
- [55] T. Bligaard, R. M. Bullock, C. T. Campbell, J. G. Chen, B. C. Gates, R. J. Gorte, C. W. Jones, W. D. Jones, J. R. Kitchin, and S. L. Scott, ACS Catalysis **6**, 2590 (2016).
- [56] N. Mardirossian and M. Head-Gordon, Molecular Physics **115**, 2315 (2017).
- [57] D. P. Tew, The Journal of Chemical Physics **145**, 074103 (2016).
- [58] E. R. Johnson and A. D. Becke, The Journal of Chemical Physics **146**, 211105 (2017).
- [59] M. Rosenblatt, The Annals of Mathematical Statistics **27**, 832 (1956).
- [60] E. Parzen, The Annals of Mathematical Statistics **33**, 1065 (1962).
- [61] M. Waskom, O. Botvinnik, D. O’Kane, P. Hobson, J. Ostblom, S. Lukauskas, D. C. Gemperline, T. Augspurger, Y. Halchenko, J. B. Cole, J. Warmenhoven, J. de Ruiter, C. Pye, S. Hoyer, J. Vanderplas, S. Villalba, G. Kunter, E. Quintero, P. Bachant, M. Martin, K. Meyer, A. Miles, Y. Ram, T. Brunner, T. Yarkoni, M. L. Williams, C. Evans, C. Fitzgerald, Brian, and A. Qalieh, “mwaskom/seaborn: v0.9.0 (July 2018),” (2018).
- [62] M. D. Brown, J. R. Trail, P. Lpez Ros, and R. J. Needs, J. Chem. Phys. **126**, 224110 (2007).
- [63] A. J. Merer, Annual Review of Physical Chemistry **40**, 407 (1989).
- [64] K. D. Carlson, E. Ludea, and C. Moser, The Journal of Chemical Physics **43**, 2408 (1965).
- [65] B. d. Darwent, Nat. Stand. Ref. Data Ser. **31**, 60 (1970).
- [66] K. D. Carlson and R. K. Nesbet, The Journal of Chemical Physics **41**, 1051 (1964).
- [67] J. Berkowitz, W. A. Chupka, and M. G. Inghram, The Journal of Chemical Physics **27**, 87 (1957).
- [68] G. Balducci, G. D. Maria, M. Guido, and V. Piacente, The Journal of Chemical Physics **55**, 2596 (1971).
- [69] D. E. Clemmer, N. F. Dalleska, and P. B. Armentrout, The Journal of Chemical Physics **95**, 7263 (1991).
- [70] M. A. L. Marques, M. J. T. Oliveira, and T. Burnus, Computer Physics Communications **183**, 2272 (2012).

I. DETAILED METHODOLOGY

A. AFQMC

The AFQMC method [1–3] estimates the ground-state properties of a many-fermion system by statistically sampling the wave function $|\psi_g\rangle \propto e^{-\beta\hat{H}}|\psi^0\rangle$, where $|\psi^0\rangle$ is an initial wave function which is nonorthogonal to the ground state. The projection is carried out iteratively by small time step $e^{-\Delta\tau\hat{H}}$, with $\beta = n\Delta\tau$ sufficiently large to project out all excited states. The propagator is represented as $e^{-\Delta\tau\hat{H}} = \int d\mathbf{x} p(\mathbf{x}) \hat{B}(\mathbf{x})$ where $\hat{B}(\mathbf{x})$ is a one-body operator which depends on the vector \mathbf{x} , and $p(\mathbf{x})$ is a probability distribution. This representation maps a many-body system into an ensemble of one-body systems, with the ensemble then sampled by Monte Carlo (MC) techniques. We use open-ended random walks in Slater determinant space to sample the imaginary time projection and represent the ground state wave function: $|\psi_g\rangle = \int d\phi c_\phi |\phi\rangle$, where the Slater determinants in the integral are non-orthogonal $\langle\phi'|\phi\rangle \neq 0$. A gauge constraint, implemented approximately with a trial wave function $|\psi_T\rangle$, is applied on the sampled Slater determinants [1, 2] to control the sign or phase problem.

In this work, we present results obtained from the AFQMC method implemented for Gaussian basis sets [4, 5]. We set the linear dependence threshold to be 10^{-8} for the one-electron basis [6] and use the modified Cholesky decomposition [7] with a threshold 10^{-6} for the Coulomb interaction. Most of the calculations use projection time $\beta = 35 E_{Ha}^{-1}$ and time step $\Delta\tau = 0.005 E_{Ha}^{-1}$. The convergence error from finite β is negligible and extrapolations are performed when the Trotter error is larger than Monte Carlo uncertainty. The reported error bars are estimated by one standard deviation statistical errors.

Truncated CASSCF wave functions were used as $|\psi_T\rangle$ here. Fast update procedure [8, 9] allows the use of multi-determinant CAS trial wave functions with sublinear cost. (For example, in ScO TZ basis, the cost of the AFQMC calculation with a $|\psi_T\rangle$ of 163 determinants is $2.1\times$ that of a single determinant calculation.) Typically around 10 CAS orbitals are used to generate the $|\psi_T\rangle$ in both atoms and molecules. Following procedures in past AFQMC calculations using CASSCF [10, 11], we truncate the wave function by discarding determinants with the smallest weights, up to an integrated weight of $\delta = 10^{-3}$, which results in ~ 100 determinants in most cases. Because of the fast update algorithm, we could check the effect on the AFQMC results of increasing the CAS space to the next level with little cost. In VO and FeO, a noticeable difference was seen outside the statistical error, and we increased the CAS space to 12, resulting in ~ 1700 and ~ 1600 determinants, respectively, in their $|\psi_T\rangle$.

In solids, CASSCF trial wave functions would not be applicable straightforwardly in a size-consistent manner. There have been many benchmark studies of AFQMC using single determinant trial wave functions (e.g. Refs. [10–12]). To give an idea of the dependence of the constraint error in AFQMC for the specific systems here, the computed total energies in TiO, VO, CrO, MnO change by about -4.9 , -1.5 , $+6.8$, and -9.7 milli-Hartrees from the reported multi-det $|\psi_T\rangle$ results when a single determinant UHF trial wave function is used (TZ basis, with MC error bars 1-2 milli-Hartrees). Besides using a single Slater determinant, there are a number of possibilities to systematically improve the trial wave function, including generalized Hartree-Fock [13], symmetry projection and symmetry-adapted multi-determinants [6, 14, 15], Hartree-Fock-Bogoliubov form [16, 17], self-consistent trial wave functions [18, 19].

B. Configuration interaction

Configuration interaction with singles and doubles excitations (CISD) was used as implemented in the PySCF package. CISD approximates the many-body wave function as a sum of Slater determinants, constructed from a reference Slater determinant, which was taken from restricted open shell Hartree-Fock. In CISD, the wave function is given as

$$\begin{aligned} |\Psi_{CISD}\rangle = & (c_0 \\ & + \sum_{ij,\sigma} C_{ai}^{(s)} c_{a,\sigma}^\dagger c_{i,\sigma} \\ & + \sum_{ijkl,\sigma,\sigma'} C_{abij,\sigma,\sigma'}^{(d)} c_{a,\sigma}^\dagger c_{b,\sigma'}^\dagger c_{i,\sigma} c_{j,\sigma'} \\ &) |\Psi_{HF}\rangle, \end{aligned}$$

where c^\dagger and c are creation/destruction operators, respectively, a, b refer to virtual orbitals, i, j refer to occupied orbitals, and all C parameters are variationally optimized. CISD scales approximately as $\mathcal{O}(N_e^6)$ and is known to not

TABLE I. Calculations in the database. In each cell, the symbols correspond to the basis performed as follows: d: vdz, t: vtz, q: vqz, 5: v5z, c: cbs. A dash means that there were no calculations for that system using that technique.

Method	System														
	Cr	Cr+	CrO	Cu	Cu+	CuO	Fe	Fe+	FeO	Mn	Mn+	MnO	O	O+	Sc
AFQMC(MD)	dtq5	dtq5	dtq5	dtq5	dtq5	dtq5	dtq5	dtq5	dtq5	dtq5	dtq5	dtq5	dtq5	dtq5	dtq5
B3LYP	dtq5	dtq5	dtq5	dtq5	dtq5	dtq5	dtq5	dtq5	dtq5	dtq5	dtq5	dtq5	dtq5	dtq5	dtq5
CISD	dtq5	dtq5	dtq5	dtq5	dtq5	dtq5	dtq5	dtq5	dtq5	dtq5	dtq5	dtq5	dtq5	dtq5	dtq5
DMC(SD)	c	c	c	c	c	c	c	c	c	c	c	c	c	c	c
DMRG	dt	dt	d	dt	dt	d	dt	dt	dt	d	dt	d	dt	dt	d
GF2	dtq	dtq	dtq	—	dtq	dtq	dtq	dtq	dtq	dtq	dtq	dtq	dtq	dtq	dtq
HF+RPA	t	t	t	t	t	—	dt	t	t	t	t	t	t	t	t
HSE06	dtq5	dtq5	dtq5	dtq5	dtq5	—	ddtq5	dtq5	dtq5	dtq5	dtq5	ddtq5q	dtq5	ddtq5q	dtq5
LDA	dtq5	dtq5	dtq5	dtq5	dtq5	dtq5	dtq5	dtq5	dtq5	dtq5	dtq5	dtq5	dtq5	dtq5	dtq5
MRLCC	dtq5	dtq5	dtq5	dtq5	dtq5	dtq5	dtq5	dtq5	dtq5	dtq5	dtq5	dtq5	dtq5	dtq5	dtq5
PBE	dtq5	dtq5	dtq5	dtq5	dtq5	dtq5	dtq5	dtq5	dtq5	dtq5	dtq5	dtq5	dtq5	dtq5	dtq5
PBE+RPA	t	t	t	t	t	—	t	t	t	t	t	t	t	t	t
QSGW	t	t	t	—	—	—	dt	t	t	t	t	t	t	t	t
SC-GW	d	d	—	—	—	—	d	d	—	d	d	d	—	d	—
SCAN	dtq5	dtq5	dtq5	dtq5	dtq5	dtq5	dtq5	dtq5	dtq5	dtq5	dtq5	dtq5	dtq5	dtq5	dtq5
SEET(FCI/GF2)	dtq	dtq	dq	—	—	dtq	dtq	dtq	dtq	dtq	dtq	dtq	dtq	dtq	dtq
SHCI	dtq5	dtq5	dtq5	dtq5	dtq5	dtq5	dtq5	dtq5	dtq5	dtq5	dtq5	dtq5	dtq5	dtq5	dtq5
UCCSD	dtq5	dtq5	dtq5	dtq5	dtq5	dtq5	dtq5	dtq5	dtq5	dtq5	dtq5	dtq5	dtq5	dtq5	dtq5
UCCSD(T)	dtq5	dtq5	dtq5	dtq5	dtq5	dtq5	dtq5	dtq5	dtq5	dtq5	dtq5	dtq5	dtq5	dtq5	dtq5
iFCIQMC	dtq	dtq	—	dtq	dtq	—	dtq	dtq	—	dtq	dtq	—	dtq	dtq	—

be size extensive.

C. Coupled Cluster

Unrestricted coupled cluster was used as implemented in the PySCF package.[20] The reference state was restricted open shell Hartree-Fock. We found that an unrestricted reference state led to worse results by values up to 10 mHa for the total energy of the molecules. In UCCSD, the wave function is approximated as

$$|\Psi_{CCSD}\rangle = e^{\hat{T}}|\Psi_{HF}\rangle, \quad (1)$$

where the \hat{T} operator contains one and two body operators. The exponential *ansatz* ensures that the technique is size extensive in contrast to CISD. UCCSD scales approximately as $\mathcal{O}(N_e^6)$ [21].

UCCSD(T) evaluates the perturbative effect of including three-body operators from a UCCSD reference, and is often called the gold standard of quantum chemistry when used for equilibrium properties. It scales approximately as $\mathcal{O}(N_e^7)$. Despite the steep formal scaling, the prefactor is quite small. Thus compared to the other accurate methods in this paper, namely, SHCI, DMRG, FCIQMC, AFQMC, and SEET, the UCCSD(T) calculations were the least expensive by a significant amount.

D. Density Functional Theory

Density functional theory (DFT) in the restricted open shell Kohn-Sham approach was used as implemented in the PySCF package.[20] Level 6 grids were used to improve the accuracy, and the resultant state was carefully checked to ensure that it was the DFT ground state, since often the self consistent field process converged to the incorrect state. The basis set error in DFT is very small, typically with less than 1 mHartree difference between the vtz and v5z basis sets. This is because the basis in DFT only has to express the occupied Kohn-Sham orbitals accurately, and is not used to describe electron correlation. Strictly speaking, the DFT energy is only comparable to the many-body solution in the complete basis set, because the functionals are designed to approximate the correlation energy in the basis set limit.

E. DMRG

The density matrix renormalization group (DMRG) [22] provides a variational ansatz for the wavefunction of the matrix product state form,

$$|\Psi\rangle = \sum_{n_1 n_2 \dots n_k} [\mathbf{A}^{n_1} \mathbf{A}^{n_2} \dots \mathbf{A}^{n_k}]_{11} |n_1 n_2 \dots n_k\rangle \quad (2)$$

where \mathbf{A}^n is a matrix of variational parameters for each orbital and $|n_1 n_2 \dots n_k\rangle$ is an occupancy vector. The above ansatz expresses the coefficient of any occupancy vector as a product of matrices, where the ‘‘bond’’ dimension of the matrix \mathbf{A}^n is $M \times M$. M may be increased until the ansatz is exact, which happens for M approximately the square root of the full Hilbert space size. The cost of the calculation using the quantum chemistry Hamiltonian with quartic interactions is proportional to $M^3 k^3 + M^2 k^4$ where k is the number of orbitals [23–26]. In a localized basis, the M required for a given accuracy scales like $e^{V^{D/D+1}}$ where V is the volume of the system and D is the dimension [27]. Thus, when extending a system along one dimension, M is independent of system size, while when extending a system along all three dimensions, the computational scaling is $e^{V^{2/3}}$. In any dimension, this is therefore a savings over full configuration interaction, which scales like e^V .

As can be seen, the ansatz requires an ordering of the orbitals and also treats all orbitals on the same footing. The latter means that in practice the DMRG is often a good ansatz relative to many methods when there are active orbitals which needed to be treated in a balanced way. However, it is inefficient when there are many doubly occupied or empty orbitals. The atoms and molecules in this system fall into this latter single-reference category. Thus we do not expect the DMRG to be especially efficient, but it serves as a near-numerically exact method to benchmark other techniques more suitable for these systems.

The DMRG calculations in this work were carried out using a spin-adapted code (a slight modification of the above ansatz) which allows us to obtain pure spin states [28]. The orbital ordering was generated by the default genetic algorithm [29]. We used the two-site variant of the DMRG and carried out calculations systematically increasing M . The largest M we used ranged from 4000 - 10000. To verify the accuracy of the energy we carried out an extrapolation in the total energy. We did this either by the standard linear extrapolation in the energy against the discarded weight in the two-site algorithm, where the DMRG energies at different M were computed by sweeping backwards from the largest M down to smaller M 's (backwards schedule) [24, 29, 30], or by extrapolating the energies of the largest M values against $1/M$. In the first case, the extrapolation error is usually reported as a fraction of the extrapolation distance between the lowest variational energy and the extrapolated energy. This extrapolated energy was consistent with the energy obtained by extrapolating against $1/M$, but in some cases the $1/M$ extrapolation was more linear, and we report that as the extrapolated energy. The DMRG energies at the largest M are variational. Where included, they provide the lowest variational energies for this benchmark.

F. FCIQMC

The FCIQMC method [31–33] directly samples the many body wavefunction by stochastic propagation of a population of discrete walkers in Slater determinant space, defined by a given single particle basis. The annihilation of walkers with anti-walkers is crucial to ensure that the average wavefunction has the correct configurational sign-structure, and can lead to a circumvention of the Fermion sign problem without uncontrolled approximations. When a determinant is occupied by a small number of walkers, it is not clear whether the determinant should be ultimately dominated by walkers or anti-walkers, and so spawning new walkers from such a determinant can cause incorrect sign information to propagate throughout the network. This problem is minimized by the systematically improvable approach of Initiator FCIQMC [34, 35], which only allows the creation of new walkers on currently unoccupied determinants, by parent walkers residing on a determinant with a population above some threshold (in this work taken to be 3 walkers). This increases the incidence of annihilation events and encourages the sign-coherent propagation of walkers, and results in a convergence to the exact wavefunction energy and properties as the number of walkers increases. Furthermore, small subspaces are identified to define a ‘trial wavefunction’ onto which the sampled wavefunction is projected to calculate the energy, as well as another small subspace in which exact propagation can occur (the semi-stochastic adaptation [36, 37]). These subspaces serve to minimize the stochastic errorbars of the estimators.

All FCIQMC calculations in this work were undertaken via the following process:

- A maximum walker population N_{walker} is chosen
- The walker population is initialized on a single determinant and then allowed to reach N_{walker}
- A short interval in imaginary time after the maximum population is reached, the trial wavefunction space is initialized by performing an exact deterministic diagonalization of the Hamiltonian in the subspace spanned by the N_{TWF} most populated determinants ($N_{\text{TWF}} \sim 200$ determinants in this work)
- At the same iteration, a subspace of the N_{SS} most populated determinants is identified and designated as the semi-stochastic space. Thereafter, the walkers residing in this subspace are exactly propagated. ($N_{\text{SS}} \sim 10,000$ determinants in this work)
- The walker population is left to evolve under initiator FCIQMC dynamics until the numerator and denominator of the trial wavefunction projected energy stabilize around a mean value
- The energy is taken to be the ratio of means of the numerator and denominator of the energy
- The stochastic error is estimated using the Flyvberg – Peterson analysis[38] for serially correlated data.

The stochastically sampled wavefunction is affected by the systematic error introduced by the initiator criterion for spawning. In order to reduce this error to within acceptable bounds, the above procedure is repeated for increasingly large values of N_{walker} until convergence of the energy estimate with respect to this parameter is achieved. This was approximately 15 million, 50 million, 100 million and 200 million walkers for the Tm/Tm⁺ vdz, vtz, vqz and TmO vdz calculations respectively[39]. This computational effort very roughly corresponds to 100 core hours per million walkers, with a maximum of $\sim 15,000$ CPU hours used in order to converge to ScO (vdz) system to small random error bars (200 million walkers).

G. Fixed node diffusion Monte Carlo

Fixed node diffusion Monte Carlo was used as implemented in the QWalk package.[40] A single determinant was generated using PySCF density functional theory in the B3LYP approximation. This determinant gave the lowest upper bound energy to the ground state. We multiplied the determinant by a 3-body Jastrow factor, which then was optimized to minimize the total energy using the linear method.[41, 42] The resultant single determinant Slater-Jastrow wave function was used as a guiding function for diffusion Monte Carlo.[43] In this method, the diffusion Monte Carlo wave function is given by

$$|\Psi_{DMC}\rangle = e^{-\tau\hat{H}}|\Psi_T\rangle, \quad (3)$$

where $|\Psi_T\rangle$ is the trial wave function, in this case the Slater-Jastrow wave function. The T-moves scheme[44] was used to ensure an upper bound to the ground state energy. Timestep errors were extrapolated out using a linear fitting process and timesteps as low as $0.0025 \text{ Hartrees}^{-1}$.

Scaling in stochastic methods is complex. To obtain the total energy with a given stochastic uncertainty, DMC(SD) scales as $\mathcal{O}(N_e^3 + \epsilon N_e^4)$. The N_e^4 cost typically does not appear until the number of electrons is more than 400-500. This method has been applied on systems with more than 1000 electrons.

We also considered more accurate trial wave functions, which can improve the fixed node error. We constructed them from SHCI wave functions by running small selected CI, and choosing the determinants with the largest weights. These weights were then reoptimized in the presence of the Jastrow factor using the linear method.[41, 42]

H. GF2

The fully self-consistent second order Green's function theory (GF2) [45–49] includes all second-order skeleton diagrams dressed with the renormalized second-order propagators and bare interactions. GF2 is formulated as a low-order approximation to the exact Luttinger-Ward (LW) functional [50] and therefore is Φ -derivable, thermodynamically consistent, and conserving [51, 52].

For transition atoms, we solve all the non-linear equations self-consistently at non-zero temperature. At each iteration, the self-energy, Green's function, and Fock matrix are updated until convergence is reached, so that the converged solution is reference-independent. Because of stability problems in the self-consistency, the calculations for transition monoxides are only done with one-shot GF2 on top of unrestricted Hartree-Fock. The self-energy, Green's function, and Fock matrix are not iterated until self-consistency. All the calculations are done on a mesh that combines a sparse power-law grid with an explicit transform based on a Legendre expansion of the self-energy. [53]

I. MRLCC

The multi-reference linearized coupled-cluster (MRLCC) is a flavor of multi-reference perturbation theory. We consider a reference wavefunction $|\Psi_0\rangle$ obtained for example from a CAS-like calculation. The out-of-active-space dynamical correlation may be added by multi-reference perturbation theory, where the expressions of the four first contributions to the energy are

$$E_0 = \langle \Psi_0 | \hat{H}_0 | \Psi_0 \rangle \quad (4)$$

$$E_1 = \langle \Psi_0 | \hat{V} | \Psi_0 \rangle \quad (5)$$

$$E_2 = \langle \Psi_0 | \hat{V} | \Psi_1 \rangle \quad (6)$$

$$E_3 = \langle \Psi_1 | \hat{V} - E_1 | \Psi_1 \rangle \quad (7)$$

and where the first order correction to the wavefunction $|\Psi_1\rangle$ obeys

$$(E_0 - \hat{H}_0)|\Psi_1\rangle = \hat{V}|\Psi_0\rangle. \quad (8)$$

In Rayleigh-Schrödinger perturbation theory, the partitioning of the Hamiltonian $\hat{H} = \hat{H}_0 + \hat{V}$ is so that $|\Psi_0\rangle$ and E_0 are the eigenvector and eigenvalue of the zeroth order Hamiltonian \hat{H}_0 . As is well known, this leaves some flexibility for the choice of \hat{H}_0 , leading to different perturbation theories having different properties: the use of the

Fock operator yields CASPT[54], and the use of the Dyall Hamiltonian[55] yields NEVPT[56, 57]. In this work, we show derivations and results for the MRLCC perturbation theory[58–61], which uses the Fink Hamiltonian[62, 63]:

$$\hat{H}_0 = \left(\sum_{mn} t_m^n \hat{E}_m^n + \sum_{mnop} v_{mn}^{op} \hat{E}_{mn}^{op} \right)_{\Delta=0}, \quad (9)$$

where the spin-free excitation operators are written with a hat, t and v are tensors, and the m, n, o, p indices refer to any molecular orbital. The notation $\Delta = 0$ indicates that only terms that do not change the number of electrons in the core, active and virtual spaces are taken into \hat{H}_0 . It follows that:

$$\hat{V} = \left(\sum_{mn} t_m^n \hat{E}_m^n + \sum_{mnop} v_{mn}^{op} \hat{E}_{mn}^{op} \right)_{\Delta \neq 0}, \quad (10)$$

and one can readily see from Eqs. (4) and (5) that the zeroth order energy is the energy of the reference wavefunction and that $E_1 = 0$, which goes to say that this zeroth order Hamiltonian is somewhat close to the exact \hat{H} and is good in the context of perturbation theory (this is also the case for NEVPT).

In the internally contracted scheme, the first order correction to the wavefunction is expressed as a sum over eight class contributions $|\Psi_1^c\rangle$ expanded on perturber wavefunctions that are connected to the reference wavefunction:

$$|\Psi_1^c\rangle = \sum_I d_I^c \hat{E}_I^c |\Psi_0\rangle, \quad (11)$$

with coefficients \mathbf{d}^c . In this representation the Fink Hamiltonian is block diagonal (and so is the Dyall Hamiltonian), and the coefficients \mathbf{d}^c in Eq. (11) are found by solving Eq. (8) subsequently for each class. Projection of Eq. (8) onto the basis of a class yields:

$$\mathbf{A}^c \mathbf{d}^c = \mathbf{S}^c \mathbf{w}^c, \quad (12)$$

with

$$A_{IJ}^c = \langle \Psi_0 | \hat{E}_I^{c\dagger} [(E_0 - \hat{H}_0), \hat{E}_J^c] | \Psi_0 \rangle \quad (13)$$

$$S_{IJ}^c = \langle \Psi_0 | \hat{E}_I^{c\dagger} \hat{E}_J^c | \Psi_0 \rangle \quad (14)$$

where realizing that $(E_0 - \hat{H}_0)|\Psi_0\rangle = 0$ allows the introduction of the commutator (see for example Ref. 61).

The terms to manipulate to compute \mathbf{A} , \mathbf{S} and E_2 , E_3 involve long strings of creation/annihilation operators, and one can use the Wick's theorem to simplify the expressions. This will result in series of tensor contractions involving one and two electron integrals (stemming from \hat{H}_0 and \hat{V}), and RDMs up to fourth order. The application of the Wick's theorem to the strings of operators is done with the “Second Quantization Algebra” symbolic algebra Python library [?], which we modified to fit our needs. The scripts also automate the generation of the C code used to solve the resulting equations and to calculate the energies E_2 and E_3 .

J. QSGW

Typically RPA total energies are done from a simple one-body reference Hamiltonian H_0 such as PBE, HSE06, or Hartree-Fock. Since different choices yield different results, there are significant and unavoidable ambiguities. First of all, there is a fundamental issue: When employing a non-self-consistent Green's function, the different formulas for the total energy do differ in practice: the Galitskii-Migal and the RPA total energies are not equal any more [64].

The starting-point dependence can be surmounted by iterating G to self-consistency, that is, by finding a G generated by GW that is the same as the G that generates it ($G^{\text{out}}=G^{\text{in}}$). But it has long been known that full self-consistency can be quite poor in solids [65, 66]. A recent re-examination of some semiconductors [67] confirms that the dielectric function (and concomitant QP levels) indeed worsen when G is self-consistent, for reasons explained in Appendix A in Ref. [68]. Fully scGW becomes more problematic in transition metals [69]. Finally, scGW is a conserving approximation in the Green's function G , but W loses its usual physical meaning as a response function.

An alternative is the Quasiparticle Self-Consistent GW approximation[70] (QSGW). It is similar to scGW, but at each cycle the dynamical self-energy is rendered static and hermitian, forming a new noninteracting G_0 by making the substitution

$$V^{\text{xc}} = \frac{1}{2} \sum_{ij} |\psi_i\rangle \{ \text{Re}[\Sigma(\varepsilon_i)]_{ij} + \text{Re}[\Sigma(\varepsilon_j)]_{ij} \} \langle \psi_j|, \quad (15)$$

where $\text{Re}\{\}$ stands for the Hermitian part of the operator. This process is carried through to self-consistency. It was formally justified [68, 70] as a construction to optimize the noninteracting Green's function G_0 by minimizing some measure of the difference $|G - G_0|$. More recently it has been justified as minimizing the the gradient of the Baym-Kadanoff functional in the space of all G_0 [71].

QSGW is nevertheless an approximate self-consistent procedure, which relies on effective one-electron wavefunctions instead of the full Green's function. As a consequence, the difference between the expressions for the total energy (Galitskii-Migdal or RPA) still persists once the self-consistency has been reached. In this work, we defined the QSGW total energy as the one obtained from the RPA expression based on QSGW eigenvalues and wavefunctions, consistently with Ref. 72. Indeed, the RPA total energy, through the adiabatic connection, is capable of incorporating the correlated part of the kinetic energy [73], whereas the Galitskii-Migdal is not. The correlated part of the kinetic energy is sizeable and it is important to include it properly.

It is well known that GW overestimates the correlation energy. A prior study of weakly correlated molecular dimers[74] showed that (1) the RPA tends to systematically overestimate the correlation energy, and (2) the error is connected with short-ranged correlations. This tendency is also found here, as noted in the main text. The ionization energy and the dimer formation energy, both of which benefit from partial cancellation of errors in short-range correlation, are much better described. We also find that the RPA total energy based on QSGW, with its optimal choice for G_0 , perform significantly better than RPA based on other G_0 , e.g. PBE or Hartree Fock, as will be shown elsewhere.

Finally, it has been established, using less optimal forms for G_0 , that low-order diagrammatic corrections (especially second order screened exchange) significantly reduce errors in the correlation energy [75, 76]. It is shown elsewhere [77] how ladders dramatically improve the dielectric function in TM oxide crystals, so it is reasonable to expect that correlation energies computed from it will see a similar improvement. Density-functional approximations for the exchange-correlation kernel significantly improve on heats of formation of dimers from *sp* elements [78].

K. RPA

We calculated the RPA total energy using the Tamm-Dancoff approximation (specifically Eq. (9) from Ref. [79]), using several flavors of G_0 : PBE, Hartree-Fock, HSE06, and QSGW, for the TM atom and M+O dimer. All the RPA calculations in this paper use the MOLGW code [80].

L. sc-GW

The GW method [81] evaluates a subset of terms of a diagrammatic weak coupling series in the interaction V deterministically. The GW approximation can be understood as a first-order approximation to Hedin's series of renormalized propagators and interactions. It is expressed in terms of self-energies Σ , Green's functions G , screened interactions W and polarizations P by the self-consistent solution of the equations $G = G_0 + G_0 \Sigma G$, $W = V + V P W$, where G_0 denotes the Hartree-Fock Green's function, and Σ and P are computed as $\Sigma = -GW$ and $P = GG$. The main difference to GF2 is that, in GW , both propagators and interactions are renormalized, whereas GF2 only renormalizes the propagators. However, GF2 obtains all second order contributions, whereas the second order exchange is missing from GW . Our results are converged to self-consistency, using a finite-temperature imaginary time formulation evaluated at temperatures low enough that the system is in its ground state. Sparse imaginary time and Matsubara frequency grids based on Chebyshev polynomials and the intermediate representation (IR) [82–84] is used, which significantly reduced the computational cost. Our code is based on the ALPS libraries [85, 86].

Self-consistent GW is a Φ - [51, 52] and Ψ -derivable [87] weak coupling method, in the sense that it neglects some diagrams of order V^2 . Achieving full self-consistency requires the storage and manipulation of W , which is a frequency-dependent four-index tensor. The necessity of handling this object numerically restricts the method in our implementation to relatively small system sizes.

M. Self-energy embedding theory (SEET)

SEET [88–95] is a finite temperature Green's function embedding method. The embedding construction allows us to describe the weakly and strongly correlated orbitals at different levels of theory. The weakly correlated orbitals are

treated by a low level, most often a perturbative method (here Green’s function second order (GF2) [46–48, 96–98] or a single iteration of GF2). The strongly correlated orbitals are treated with a high level, usually non-perturbative method. When multiple strongly correlated orbitals are present, they are separated into several intersecting or non intersecting subsets A_i . Each of these subsets contains M_i^A orbitals and $M = \sum_i M_i^A + M^R$, where M is the total number of orbitals in the problem and M^R are all the orbitals that are not contained in the groups of the strongly correlated orbitals. The orbitals from each of the subsets A_i are used to construct Anderson Impurity Models (AIM) that are then solved by a non-perturbative method, here full configuration interaction (FCI) [99–101]. The intersubset interactions are treated most commonly at a perturbative level. Orbitals chosen to each of the A_i subsets can be chosen based on several criteria such as occupancies of natural orbitals (NOs) or energies of molecular orbitals (MOs), for details see Refs. [48,50].

A general SEET functional can be written as

$$\begin{aligned} \Phi_{\text{MIX}}^{\text{SEET}} = & \Phi_{\text{weak}}^{\text{tot}} + \sum_i \binom{n}{k} (\Phi_{\text{strong}}^{A_i^k} - \Phi_{\text{weak}}^{A_i^k}) \\ & \pm \sum_{k=K-1}^{k=1} \sum_i \binom{n}{k} (\Phi_{\text{strong}}^{B_i^k} - \Phi_{\text{weak}}^{B_i^k}), \end{aligned} \quad (16)$$

where $\Phi_{\text{weak}}^{\text{tot}}$, in this work is a GF2 solution for the whole orbital space, $\Phi_{\text{strong}}^{A_i^k}$ is obtained from the solution of AIM for the strongly correlated subset of orbitals A_i , $\Phi_{\text{weak}}^{A_i^k}$ is the solution of the subset A_i with a weakly correlated method used to remove the double counting. The terms $(\Phi_{\text{strong}}^{B_i^k} - \Phi_{\text{weak}}^{B_i^k})$ are present in case of intersecting subsets A_i and are necessary to remove the double counting, for details see Ref. 93. We denote a particular SEET calculation as SEET(method strong/method weak)-m([M^AO]/basis) since self-energies from intersecting orbital subspaces containing M^A orbitals are treated with “method strong”. The whole system is treated with “method weak” and the orbitals from subsets A_i are transformed to a certain orbital basis denoted here as “basis”. In this paper, we most commonly use the basis of molecular orbitals. The details of the finite temperature imaginary time GF2 grid as well as the frequency grid can be found in Ref. 53, 102, and 103.

N. SHCI

The semistochastic heat-bath configuration iteration (SHCI) method [104–107], is an efficient instance of the general class of methods wherein a selected configuration interaction is performed followed by a perturbative correction (SCI+PT). SCI+PT methods have two stages. In the first stage a set of “important” determinants are selected the Hamiltonian is diagonalized in the subspace of these determinants, \mathcal{V} , to obtain the the lowest few eigenstates (or the lowest state if one is interested in the ground state only). In the second stage, a second-order perturbation theory is used to calculate the energy contributions of all determinants that do not belong to the space \mathcal{V} but have a non-zero Hamiltonian matrix element with at least one of the determinants in \mathcal{V} . Such methods have been used for about 50 years [108–110] and continue to be a subject of interest [111–119] to the present day.

We briefly describe the two innovations that account for the time- and memory-efficiency of SHCI. A more detailed description can be found in 107.

1. During the variational and the perturbative steps, straightforward implementations of SCI+PT scan all determinants connected to at least one of the determinants in \mathcal{V} and select those determinants ($|D_a\rangle$) for which the absolute value of the 2^{nd} -order perturbative contribution to the energy

$$\left| \frac{(\sum_{D_i \in \mathcal{V}} H_{ai} c_i)^2}{E_V - E_a} \right| > \epsilon, \quad (17)$$

where the subscript a denotes a determinant not currently present in \mathcal{V} , E_V is the energy of the current variational wavefunction, E_a is the energy of determinant D_a , and ϵ is a parameter that controls the number of determinants selected. During the variational stage, this is done iteratively to build up the variational wavefunction starting from a single determinant. During the perturbative stage, $\epsilon = 0$. Instead, SHCI modifies the selection criterion to [104],

$$\max_{D_i \in \mathcal{V}} |H_{ai} c_i| > \epsilon, \quad (18)$$

which greatly reduces the cost by taking advantage of the fact that most of the matrix elements, H_{ai} , are 2-body excitations, which depend only on the indices of the 4 orbitals whose occupations change and not on the other

occupied orbitals of a determinant. Thus by presorting the absolute values of all possible matrix elements of the 2-body excitations in descending order, the scan over determinants D_a can be terminated when $|H_{ai}|$ drops below ϵ/c_i . A similar idea is used to speed up the selection of 1-body excitations as well. This enables a procedure in which *only the important determinants which will be included in the variational wavefunction, or make significant contributions to the perturbative correction, are ever looked at*, resulting in orders of magnitude saving over a naive implementation of the SCI+PT algorithm! Different values of ϵ are used during the variational and the perturbative stages of the calculation, which we denote by ϵ_1 and ϵ_2 .

2. The first innovation greatly speeds up both the variational and the perturbative steps of the algorithm. However, the perturbative step has a very large memory requirement when \mathcal{V} has a large number of determinants (say 10^9) because all determinants that are connected to those in \mathcal{V} must be stored. [120] We have developed a 2-step [105] and later a 3-step [107] semistochastic perturbative approach that both completely overcomes this memory bottleneck and is faster than the deterministic approach.

In addition to these two major methodological improvements, the SHCI method uses auxiliary arrays to speed up the computation of the Hamiltonian matrix [107]. Further, it makes extensive use of hashing and techniques such as variable-byte encoding, hardware atomic operations, dynamic load-balancing and thread pooling to achieve a high efficiency in the use of computer time and memory.

The convergence of the variational and perturbative energies depends significantly on the orbitals used. The convergence obtained from using Hartree-Fock orbitals can be improved by using natural orbitals obtained from an SHCI calculation with a fairly large value of ϵ_1 , and can be further improved by using orbitals that minimize the SHCI variational energy using a modified version of the algorithm described in Ref. 121.

We typically choose $\epsilon_2 = 10^{-6}\epsilon_1$, so that a single parameter, ϵ_1 controls the accuracy of the calculation. The energy at the $\epsilon_1 = 0$ limit is obtained using a quadratic fit to the energies versus the perturbative correction [106]. Note that although the SHCI algorithm has a perturbative component, systematically improvable approximations to the exact energy in the chosen basis are obtained by performing calculations with progressively smaller values of ϵ_1 until the total energy (variational energy plus perturbative correction), or its extrapolation versus the perturbative correction, is converged to the desired tolerance.

II. BASIS SETS, BOND LENGTHS, AND EFFECTIVE CORE POTENTIALS

All calculations used the effective core potentials and associated aug-ccpVnZ gaussian basis sets of Trail and Needs[122–124]. These effective core potentials are produced from explicitly correlated multi-configuration Hartree-Fock calculations, and include contributions from core-core and core-valence correlations. Augmented double-, triple-, quadruple-, and quintuple-zeta basis sets were used.

The molecules were computed with bond lengths in Å as follows: ScO: 1.668, TiO: 1.623, VO: 1.591, CrO: 1.621, MnO: 1.648, FeO: 1.616, CuO: 1.725.

III. DATA

Each contributing author provided a separate data file detailing the results of their calculations for both atomic and molecular systems. Each row of each data file indicates the system considered, the method and the basis set used, and the resulting total energies, along with any associated systematic or stochastic error. Additional method-specific information is also included (for example, the size of the active orbital space used in auxiliary-field quantum Monte Carlo). Not all methods completed each calculation using each level of basis set quality, due to the high computational expense of some methods.

The CSV headers required are:

- charge: charge of the molecule/atom (either 0 or 1)
- molecule: (for molecules) the name of the molecule: example “VO”
- atom: (for atoms) the name of the atom: example “V”
- pseudopotential: always “trail” for this test set

- pyscf-version: “new” for after pyscf 1.5. A small improvement in accuracy was implemented after this version. Should be “new” for all calculations
- method: a string representing the method used for the calculation. example “PBE”
- totalenergy: total energy in Hartrees
- totalenergy-stocherr : Stochastic error estimate
- totalenergy-syserr : Systematic error estimate, if available

A script called ‘gather.py’ retrieves all data from all directories. Further scripts handle plotting and error estimation.

IV. ENERGY COMPARISON FOR SEVERAL ACCURATE METHODS

There are 5 methods (DMRG, iFCIQMC, UCCSD(T), AFQMC(MD) and SEET(FCI/GF2)) for which the total energies have an rms deviation of 4 mHa or less relative to the SHCI reference. The maximum absolute error, the rms error and the number of systems treated are shown in Table IV for these methods. Tables IV and IV show the corresponding quantities for the ionization energy and the dissociation energy.

TABLE II. Total energy errors relative to SHCI of the five methods that agree best with SHCI.

Method	# systems	max abs error	rms error
DMRG	39	0.001010	0.000238
iFCIQMC	49	0.001611	0.000639
UCCSD(T)	92	0.006811	0.002309
AFQMC(MD)	92	0.007470	0.003540
SEET(FCI/GF2)	59	0.013656	0.004001

TABLE III. Ionization energy errors relative to SHCI of the five methods that agree best with SHCI.

Method	# systems	max abs error	rms error
DMRG	14	0.000826	0.000307
iFCIQMC	21	0.000965	0.000567
UCCSD(T)	28	0.001222	0.000675
AFQMC(MD)	28	0.008400	0.002888
SEET(FCI/GF2)	18	0.006580	0.002466

TABLE IV. Dissociation energy errors relative to SHCI of the five methods that agree best with SHCI.

Method	# systems	max abs error	rms error
DMRG	7	0.000678	0.000327
iFCIQMC	1	0.000488	0.000488
UCCSD(T)	28	0.005108	0.002990
AFQMC(MD)	28	0.007880	0.002590
SEET(FCI/GF2)	14	0.008356	0.004152

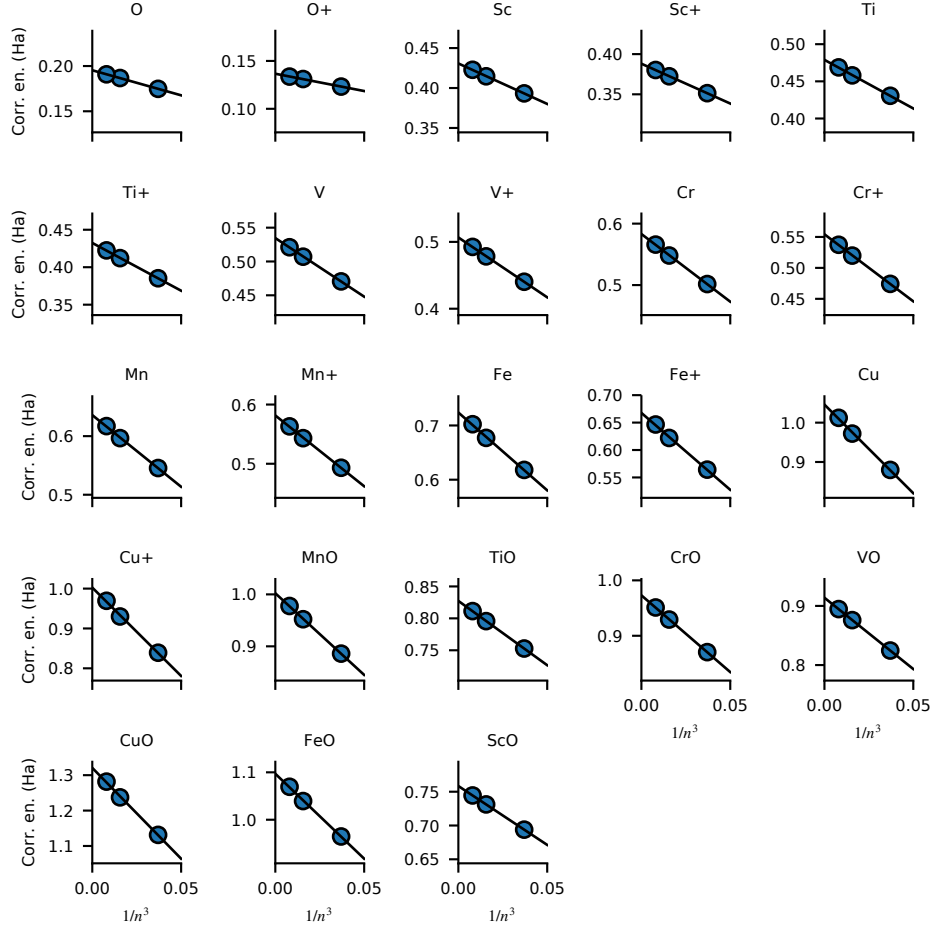


FIG. 1. Basis set extrapolation of the SHCI correlation energy versus the n in the basis vnz . Only n values from 3-5 are shown since the $n = 2$ points deviate significantly from the straight lines shown.

V. BASIS SET EXTRAPOLATION

Methods not operating directly in the complete basis set limit must be extrapolated using finite basis calculations. The extrapolated energy $E_m(\text{CBS})$ for method m is estimated from

$$E_m(\text{CBS}) = E_{\text{HF}}(\text{CBS}) + \Delta(\text{CBS}). \quad (19)$$

where $E_{\text{HF}}(\text{CBS})$ is obtained by fitting the HF energies to the form

$$E_{\text{HF}}(n) = E_{\text{HF}}(\text{CBS}) + b \exp(-cn). \quad (20)$$

and $\Delta(\text{CBS})$ is obtained by fitting the correlation energies to

$$E_m(n) - E_{\text{HF}}(n) = \Delta(\text{CBS}) + \frac{\gamma}{n^3}, \quad (21)$$

where n is the cardinal index of the basis.

An example extrapolation for all materials and SHCI correlation energies is shown in Fig 1. Extrapolations for the total energy, ionization energy and dissociation energy are shown in Tables V, VI and VII respectively. The ionization and dissociation energies converge much more rapidly than the total energies. Of the 4 basis set extrapolations considered, cbs45 is the most accurate. Table VIII shows the rms deviation of the total, ionization and binding energies of each basis set and extrapolation relative to the corresponding cbs45 energies.

TABLE V. SHCI total energies for all basis sets and extrapolations. cbs23 indicates an extrapolation using only vdz and vtz bases, and cbs34/cbs45/cbs345 are labeled in the same way. The differences between the cbs345 and the cbs45 extrapolations increase with the atomic number of the transition metal and range from 1-8 mHa. The cbs45 extrapolation is the most accurate one.

Total Energy (Ha)								
basis	O	Sc	Ti	V	Cr	Mn	Fe	Cu
vdz	-15.781250	-46.396850	-57.883050	-71.077670	-86.612030	-103.942260	-123.518120	-197.236900
vtz	-15.827020	-46.452300	-57.954630	-71.168980	-86.720920	-104.063660	-123.657200	-197.444640
vqz	-15.839090	-46.474000	-57.983000	-71.205780	-86.767610	-104.115010	-123.716750	-197.536420
v5z	-15.843170	-46.482130	-57.993860	-71.219830	-86.785320	-104.135420	-123.741800	-197.576080
cbs23	-15.846068	-46.475646	-57.985016	-71.207033	-86.766697	-104.114189	-123.715147	-197.531655
cbs34	-15.847828	-46.489701	-58.003293	-71.232489	-86.801544	-104.152337	-123.760024	-197.603262
cbs345	-15.847658	-46.490126	-58.004201	-71.233375	-86.802563	-104.154264	-123.763441	-197.609436
cbs45	-15.847432	-46.490691	-58.005411	-71.234555	-86.803920	-104.156833	-123.767993	-197.617661
Total Energy (Ha)								
basis	O+	Sc+	Ti+	V+	Cr+	Mn+	Fe+	Cu+
vdz	-15.300670	-46.156830	-57.634020	-70.828400	-86.372410	-103.673360	-123.233540	-196.967230
vtz	-15.333580	-46.211490	-57.704240	-70.919550	-86.472980	-103.792140	-123.368570	-197.163040
vqz	-15.342100	-46.233110	-57.732560	-70.957590	-86.518670	-103.842720	-123.427090	-197.253430
v5z	-15.344790	-46.241150	-57.743160	-70.971820	-86.536270	-103.862840	-123.451830	-197.292510
cbs23	-15.348503	-46.234171	-57.733836	-70.957555	-86.515427	-103.840708	-123.424132	-197.245135
cbs34	-15.348554	-46.248705	-57.752710	-70.985120	-86.552131	-103.879380	-123.469470	-197.319302
cbs345	-15.348317	-46.248980	-57.753325	-70.985640	-86.553226	-103.881194	-123.472883	-197.325395
cbs45	-15.348001	-46.249346	-57.754146	-70.986333	-86.554685	-103.883611	-123.477431	-197.333514
Total Energy (Ha)								
basis	ScO	TiO	VO	CrO	MnO	FeO	CuO	
vdz	-62.420040	-73.903750	-87.085770	-102.558370	-119.850510	-139.435990	-213.123030	
vtz	-62.530130	-74.030850	-87.235260	-102.718670	-120.029280	-139.635460	-213.377780	
vqz	-62.568454	-74.075488	-87.288682	-102.779756	-120.097071	-139.711352	-213.484244	
v5z	-62.582141	-74.091473	-87.307394	-102.802737	-120.122364	-139.741682	-213.529128	
cbs23	-62.576098	-74.084170	-87.297330	-102.786429	-120.103370	-139.717990	-213.483952	
cbs34	-62.595849	-74.107270	-87.326938	-102.823579	-120.145888	-139.766095	-213.561561	
cbs345	-62.596114	-74.107694	-87.326918	-102.824937	-120.147133	-139.769181	-213.567787	
cbs45	-62.596466	-74.108258	-87.326891	-102.826745	-120.148791	-139.773293	-213.576082	

TABLE VI. SHCI ionization energies. cbs23 indicates an extrapolation using only vdz and vtz bases, and cbs34/cbs45/cbs345 are labeled in the same way. Experimental values are also shown.

Ionization Potential (Ha)							
basis	Sc	Ti	V	Cr	Mn	Fe	Cu
vdz	0.240020	0.249030	0.249270	0.239620	0.268900	0.284580	0.269670
vtz	0.240810	0.250390	0.249430	0.247940	0.271520	0.288630	0.281600
vqz	0.240890	0.250440	0.248190	0.248940	0.272290	0.289660	0.282990
v5z	0.240980	0.250700	0.248010	0.249050	0.272580	0.289970	0.283570
cbs23	0.241474	0.251180	0.249479	0.251269	0.273481	0.291015	0.286520
cbs34	0.240996	0.250583	0.247369	0.249413	0.272957	0.290555	0.283961
cbs345	0.241146	0.250876	0.247735	0.249337	0.273071	0.290558	0.284041
cbs45	0.241346	0.251265	0.248222	0.249235	0.273222	0.290562	0.284147
exper	0.24113	0.25093	0.24792	0.24866	0.27320	0.29041	0.28394

TABLE VII. SHCI dissociation energies for the molecules considered in this work. cbs23 indicates an extrapolation using only vdz and vtz bases, and cbs34/cbs45/cbs345 are labeled in the same way.

basis	Dissociation Energy (Ha)						
	ScO	TiO	VO	CrO	MnO	FeO	CuO
vdz	0.241940	0.239450	0.226850	0.165090	0.127000	0.136620	0.104880
vtz	0.250810	0.249200	0.239260	0.170730	0.138600	0.151240	0.106120
vqz	0.255364	0.253398	0.243812	0.173056	0.142971	0.155512	0.108734
v5z	0.256841	0.254443	0.244394	0.174247	0.143774	0.156712	0.109878
cbs23	0.254384	0.253086	0.244229	0.173665	0.143113	0.156775	0.106230
cbs34	0.258321	0.256149	0.246622	0.174208	0.145724	0.158243	0.110471
cbs345	0.258330	0.255835	0.245885	0.174716	0.145210	0.158082	0.110693
cbs45	0.258343	0.255415	0.244903	0.175394	0.144526	0.157868	0.110989

TABLE VIII. RMS deviations of the SHCI total, ionization, and dissociation energies for various basis sets and extrapolations with respect to the cbs45 extrapolation.

basis	Total energy	RMS Deviation (Ha)	
		Ionization energy	Dissociation energy
vdz	0.169949	0.007215	0.015820
vtz	0.075498	0.001572	0.005997
vqz	0.034565	0.000756	0.002160
v5z	0.017665	0.000482	0.001063
cbs23	0.036296	0.001290	0.002683
cbs34	0.005110	0.000455	0.000981
cbs345	0.002919	0.000260	0.000561

-
- [1] S. Zhang, J. Carlson, and J. E. Gubernatis, Phys. Rev. B **55**, 7464 (1997).
 - [2] S. Zhang and H. Krakauer, Phys. Rev. Lett. **90**, 136401 (2003).
 - [3] S. Zhang, *Auxiliary-Field Quantum Monte Carlo for Correlated Electron Systems*, Vol. 3 of *Emergent Phenomena in Correlated Matter: Modeling and Simulation*, Ed. E. Pavarini, E. Koch, and U. Schollwöck (Verlag des Forschungszentrum Jülich, 2013).
 - [4] W. A. Al-Saidi, S. Zhang, and H. Krakauer, The Journal of Chemical Physics **124**, 224101 (2006), <https://doi.org/10.1063/1.2200885>.
 - [5] M. Motta and S. Zhang, Wiley Interdisciplinary Reviews: Computational Molecular Science **8**, e1364 (2018), <https://onlinelibrary.wiley.com/doi/pdf/10.1002/wcms.1364>.
 - [6] M. Motta, D. M. Ceperley, G. K.-L. Chan, J. A. Gomez, E. Gull, S. Guo, C. A. Jiménez-Hoyos, T. N. Lan, J. Li, F. Ma, A. J. Millis, N. V. Prokof'ev, U. Ray, G. E. Scuseria, S. Sorella, E. M. Stoudenmire, Q. Sun, I. S. Tupitsyn, S. R. White, D. Zgid, and S. Zhang (Simons Collaboration on the Many-Electron Problem), Phys. Rev. X **7**, 031059 (2017).
 - [7] W. Purwanto, S. Zhang, and H. Krakauer, The Journal of Chemical Physics **142**, 064302 (2015), <https://doi.org/10.1063/1.4906829>.
 - [8] H. Shi and S. Zhang, *To be published*.
 - [9] J. Shee, E. J. Arthur, S. Zhang, D. R. Reichman, and R. A. Friesner, Journal of Chemical Theory and Computation **14**, 4109 (2018), pMID: 29897748, <https://doi.org/10.1021/acs.jctc.8b00342>.
 - [10] W. A. Al-Saidi, S. Zhang, and H. Krakauer, The Journal of Chemical Physics **127**, 144101 (2007), <https://doi.org/10.1063/1.2770707>.
 - [11] W. Purwanto, S. Zhang, and H. Krakauer, The Journal of Chemical Physics **142**, 064302 (2015), <https://doi.org/10.1063/1.4906829>.
 - [12] W. Purwanto, S. Zhang, and H. Krakauer, The Journal of Chemical Physics **144**, 244306 (2016), <https://doi.org/10.1063/1.4954245>.
 - [13] M. Qin, H. Shi, and S. Zhang, Phys. Rev. B **94**, 085103 (2016).
 - [14] H. Shi and S. Zhang, Phys. Rev. B **88**, 125132 (2013).
 - [15] H. Shi, C. A. Jiménez-Hoyos, R. Rodríguez-Guzmán, G. E. Scuseria, and S. Zhang, Phys. Rev. B **89**, 125129 (2014).
 - [16] H. Shi, S. Chiesa, and S. Zhang, Phys. Rev. A **92**, 033603 (2015).
 - [17] H. Shi and S. Zhang, Phys. Rev. B **95**, 045144 (2017).
 - [18] M. Qin, H. Shi, and S. Zhang, Phys. Rev. B **94**, 235119 (2016).
 - [19] Y.-Y. He, M. Qin, H. Shi, Z.-Y. Lu, and S. Zhang, arXiv e-prints , arXiv:1811.07290 (2018), arXiv:1811.07290 [cond-mat.str-el].
 - [20] Q. Sun, T. C. Berkelbach, N. S. Blunt, G. H. Booth, S. Guo, Z. Li, J. Liu, J. D. McClain, E. R. Sayfutyarova, S. Sharma, S. Wouters, and G. K.-L. Chan, Wiley Interdisciplinary Reviews: Computational Molecular Science **8**, e1340.
 - [21] R. J. Bartlett and M. Musia, Reviews of Modern Physics **79**, 291 (2007).
 - [22] S. R. White, Physical review letters **69**, 2863 (1992).
 - [23] S. R. White and R. L. Martin, The Journal of chemical physics **110**, 4127 (1999).
 - [24] G. K.-L. Chan and M. Head-Gordon, J. Chem. Phys. **116**, 4462 (2002).
 - [25] S. Keller and M. Reiher, The Journal of chemical physics **144**, 134101 (2016).
 - [26] G. K.-L. Chan, A. Keselman, N. Nakatani, Z. Li, and S. R. White, The Journal of chemical physics **145**, 014102 (2016).
 - [27] J. Hachmann, W. Cardoen, and G. K.-L. Chan, The Journal of chemical physics **125**, 144101 (2006).
 - [28] S. Sharma and G. K.-L. Chan, The Journal of chemical physics **136**, 124121 (2012).
 - [29] R. Olivares-Amaya, W. Hu, N. Nakatani, S. Sharma, J. Yang, and G. K.-L. Chan, The Journal of chemical physics **142**, 034102 (2015).
 - [30] Ö. Legeza and G. Fáth, Physical Review B **53**, 14349 (1996).
 - [31] G. H. Booth, A. J. W. Thom, and A. Alavi, The Journal of Chemical Physics **131**, 054106 (2009), <https://aip.scitation.org/doi/pdf/10.1063/1.3193710>.
 - [32] G. H. Booth, A. Grüneis, G. Kresse, and A. Alavi, Nature **493**, 365 (2013).
 - [33] G. H. Booth, S. D. Smart, and A. Alavi, Molecular Physics **112**, 1855 (2014).
 - [34] D. Cleland, G. H. Booth, and A. Alavi, The Journal of Chemical Physics **132**, 041103 (2010), <https://doi.org/10.1063/1.3302277>.
 - [35] G. H. Booth, D. M. Cleland, A. J. W. Thom, and A. Alavi, J. Chem. Phys. **135**, 084104 (2011).
 - [36] N. S. Blunt, S. D. Smart, J. A. F. Kersten, J. S. Spencer, G. H. Booth, and A. Alavi, The Journal of Chemical Physics **142**, 184107 (2015), <https://doi.org/10.1063/1.4920975>.
 - [37] F. R. Petruzielo, A. A. Holmes, H. J. Changlani, M. P. Nightingale, and C. J. Umrigar, Phys. Rev. Lett. **109**, 230201 (2012).
 - [38] H. Flyvbjerg and H. G. Petersen, The Journal of Chemical Physics **91**, 461 (1989), <https://doi.org/10.1063/1.457480>.
 - [39] R. E. Thomas, G. H. Booth, and A. Alavi, Phys. Rev. Lett. **114**, 033001 (2015).
 - [40] L. K. Wagner, M. Bajdich, and L. Mitas, Journal of Computational Physics **228**, 3390 (2009).
 - [41] J. Toulouse and C. J. Umrigar, J. Chem. Phys. **126** (2007), 10.1063/1.2437215.
 - [42] J. Toulouse and C. J. Umrigar, The Journal of Chemical Physics **128**, 174101 (2008).

- [43] W. M. C. Foulkes, L. Mitas, R. J. Needs, and G. Rajagopal, *Reviews of Modern Physics* **73**, 33 (2001).
- [44] M. Casula, *Physical Review B* **74** (2006), 10.1103/PhysRevB.74.161102.
- [45] J. J. Phillips and D. Zgid, *The Journal of Chemical Physics* **140**, 241101 (2014), <https://doi.org/10.1063/1.4884951>.
- [46] A. A. Rusakov and D. Zgid, *The Journal of Chemical Physics* **144**, 054106 (2016), <https://doi.org/10.1063/1.4940900>.
- [47] J. J. Phillips, A. A. Kananenka, and D. Zgid, *J. Chem. Phys.* **142**, 194108 (2015), <http://dx.doi.org/10.1063/1.4921259>.
- [48] A. R. Welden, A. A. Rusakov, and D. Zgid, *J. Chem. Phys.* **145**, 204106 (2016).
- [49] N. E. Dahlen and U. von Barth, *The Journal of Chemical Physics* **120**, 6826 (2004), <https://doi.org/10.1063/1.1650307>.
- [50] J. M. Luttinger and J. C. Ward, *Phys. Rev.* **118**, 1417 (1960).
- [51] G. Baym and L. P. Kadanoff, *Phys. Rev.* **124**, 287 (1961).
- [52] G. Baym, *Phys. Rev.* **127**, 1391 (1962).
- [53] A. A. Kananenka, A. R. Welden, T. N. Lan, E. Gull, and D. Zgid, *Journal of Chemical Theory and Computation* **12**, 2250 (2016), pMID: 27049642.
- [54] J. Finley, P. ke Malmqvist, B. O. Roos, and L. Serrano-Andrs, *Chemical Physics Letters* **288**, 299 (1998).
- [55] K. G. Dyall, *The Journal of Chemical Physics* **102**, 4909 (1995).
- [56] C. Angeli, R. Cimiraglia, S. Evangelisti, T. Leininger, and J.-P. Malrieu, *The Journal of Chemical Physics* **114**, 10252 (2001).
- [57] C. Angeli, R. Cimiraglia, and J.-P. Malrieu, *The Journal of Chemical Physics* **117**, 9138 (2002).
- [58] S. Sharma and A. Alavi, *The Journal of Chemical Physics* **143**, 102815 (2015).
- [59] S. Sharma, G. Jeanmairet, and A. Alavi, *The Journal of Chemical Physics* **144**, 034103 (2016).
- [60] G. Jeanmairet, S. Sharma, and A. Alavi, *The Journal of Chemical Physics* **146**, 044107 (2017).
- [61] S. Sharma, G. Knizia, S. Guo, and A. Alavi, *Journal of Chemical Theory and Computation* **13**, 488 (2017).
- [62] R. F. Fink, *Chemical Physics Letters* **428**, 461 (2006).
- [63] R. F. Fink, *Chemical Physics* **356**, 39 (2009).
- [64] N. E. Dahlen, R. van Leeuwen, and U. von Barth, *Phys. Rev. A* **73**, 012511 (2006).
- [65] E. L. Shirley, *Phys. Rev. B* **54**, 7758 (1996).
- [66] B. Holm and U. von Barth, *Phys. Rev. B* **57**, 2108 (1998).
- [67] M. Grumet, P. Liu, M. Kaltak, J. Klimeš, and G. Kresse, *Phys. Rev. B* **98**, 155143 (2018).
- [68] T. Kotani, M. van Schilfgaarde, and S. V. Faleev, *Phys. Rev. B* **76**, 165106 (2007).
- [69] K. D. Belashchenko, V. P. Antropov, and N. E. Zein, *Phys. Rev. B* **73**, 073105 (2006).
- [70] S. V. Faleev, M. van Schilfgaarde, and T. Kotani, *Phys. Rev. Lett.* **93**, 126406 (2004).
- [71] S. Ismail-Beigi, *J. Phys.: Condens. Matter* **29**, 385501 (2017).
- [72] F. Bruneval, *J. Chem. Phys.* **136**, 194107 (2012).
- [73] M. Fuchs, Y.-M. Niquet, X. Gonze, and K. Burke, *The Journal of Chemical Physics* **122**, 094116 (2005), <https://doi.org/10.1063/1.1858371>.
- [74] T. Olsen and K. S. Thygesen, *Phys. Rev. B* **86**, 081103 (2012).
- [75] X. Ren, N. Marom, F. Caruso, M. Scheffler, and P. Rinke, *Phys. Rev. B* **92**, 081104 (2015).
- [76] E. Maggio and G. Kresse, *Journal of Chemical Theory and Computation* **13**, 4765 (2017), <https://doi.org/10.1021/acs.jctc.7b00586>.
- [77] B. Cunningham, M. Grüning, P. Azarhoosh, D. Pashov, and M. van Schilfgaarde, *Phys. Rev. Mater.* **2**, 034603 (2018).
- [78] P. Liu, B. Kim, X.-Q. Chen, D. D. Sarma, G. Kresse, and C. Franchini, *Phys. Rev. Materials* **2**, 075003 (2018).
- [79] H. Eshuisa, J. Yarkony, and F. Furche, *J. Chem. Phys.* **132**, 234114 (2010).
- [80] F. Bruneval, T. Rangel, S. Hamed, M. Shao, C. Yang, and J. Neaton, *Comput. Phys. Commun.* **208**, 149 (2016).
- [81] L. Hedin, *Phys. Rev.* **139**, A796 (1965).
- [82] E. Gull, S. Isakov, I. Krivenko, A. A. Rusakov, and D. Zgid, *Phys. Rev. B* **98**, 075127 (2018).
- [83] H. Shinaoka, J. Otsuki, M. Ohzeki, and K. Yoshimi, *Physical Review B* **96**, 035147 (2017).
- [84] J. Li, M. Wallerberger, N. Chikano, C.-N. Yeh, E. Gull, and H. Shinaoka, *arXiv preprint arXiv:1908.07575* (2019).
- [85] A. Gaenko, A. Antipov, G. Carcassi, T. Chen, X. Chen, Q. Dong, L. Gamper, J. Gukelberger, R. Igarashi, S. Isakov, M. Könz, J. LeBlanc, R. Levy, P. Ma, J. Paki, H. Shinaoka, S. Todo, M. Troyer, and E. Gull, *Computer Physics Communications* **213**, 235 (2017).
- [86] M. Wallerberger, S. Isakov, A. Gaenko, J. Kleinhenz, I. Krivenko, R. Levy, J. Li, H. Shinaoka, S. Todo, T. Chen, X. Chen, J. P. F. LeBlanc, J. E. Paki, H. Terletska, M. Troyer, and E. Gull, *arXiv e-prints*, arXiv:1811.08331 (2018), arXiv:1811.08331 [physics.comp-ph].
- [87] C.-O. ALMBLADH, U. V. BARTH, and R. V. LEEUWEN, *International Journal of Modern Physics B* **13**, 535 (1999), <https://doi.org/10.1142/S0217979299000436>.
- [88] D. Zgid and E. Gull, *New J. Phys.* **19**, 023047 (2017).
- [89] A. A. Kananenka, E. Gull, and D. Zgid, *Phys. Rev. B* **91**, 121111 (2015).
- [90] T. N. Lan, A. A. Kananenka, and D. Zgid, *J. Chem. Phys.* **143**, 241102 (2015), <http://dx.doi.org/10.1063/1.4938562>.
- [91] T. Nguyen Lan, A. A. Kananenka, and D. Zgid, *J. Chem. Theory Comput.* **12**, 4856 (2016).
- [92] T. N. Lan, A. Shee, J. Li, E. Gull, and D. Zgid, *Phys. Rev. B* **96**, 155106 (2017).
- [93] T. N. Lan and D. Zgid, *J. Phys. Chem. Lett.* **8**, 2200 (2017), pMID: 28453934, <http://dx.doi.org/10.1021/acs.jpclett.7b00689>.
- [94] L. N. Tran, S. Isakov, and D. Zgid, *J. Phys. Chem. Lett.* **9**, 4444 (2018), pMID: 30024163.
- [95] A. A. Rusakov, S. Isakov, L. N. Tran, and D. Zgid, *J. Chem. Theory Comput.* **15**, 229 (2019), <https://doi.org/10.1021/acs.jctc.8b00927>.

- [96] J. J. Phillips and D. Zgid, *J. Chem. Phys.* **140**, 241101 (2014), <http://dx.doi.org/10.1063/1.4884951>.
- [97] D. Neuhauser, R. Baer, and D. Zgid, *ArXiv e-prints* (2016), arXiv:1603.04141 [physics.chem-ph].
- [98] A. A. Kananenka and D. Zgid, *J. Chem. Theory Comput.* **13**, 5317 (2017), <https://doi.org/10.1021/acs.jctc.7b00701>.
- [99] D. Zgid and G. K.-L. Chan, *J. Chem. Phys.* **134**, 094115 (2011), <http://dx.doi.org/10.1063/1.3556707>.
- [100] D. Zgid, E. Gull, and G. K.-L. Chan, *Phys. Rev. B* **86**, 165128 (2012).
- [101] D. Medvedeva, S. Iskakov, F. Krien, V. V. Mazurenko, and A. I. Lichtenstein, *Phys. Rev. B* **96**, 235149 (2017).
- [102] E. Gull, S. Iskakov, I. Krivenko, A. A. Rusakov, and D. Zgid, *Phys. Rev. B* **98**, 075127 (2018).
- [103] A. A. Kananenka, E. Gull, and D. Zgid, *Phys. Rev. B* **91**, 121111 (2015).
- [104] A. A. Holmes, N. M. Tubman, and C. J. Umrigar, *J. Chem. Theory Comput.* **12**, 3674 (2016).
- [105] S. Sharma, A. A. Holmes, G. Jeanmairet, A. Alavi, and C. J. Umrigar, *J. Chem. Theory Comput.* **13**, 1595 (2017).
- [106] A. A. Holmes, C. J. Umrigar, and S. Sharma, *J. Chem. Phys.* **147** (2017).
- [107] J. Li, M. Otten, A. A. Holmes, S. Sharma, and C. J. Umrigar, *J. Chem. Phys.* **148**, 214110 (2018).
- [108] C. F. Bender and E. R. Davidson, *Phys. Rev.* **183**, 23 (1969).
- [109] B. Huron, J. Malrieu, and P. Rancurel, *J. Chem. Phys.* **58**, 5745 (1973).
- [110] R. J. Buenker and S. D. Peyerimhoff, *Theor. Chim. Acta* **35**, 33 (1974).
- [111] F. A. Evangelista, *J. Chem. Phys.* **140**, 124114 (2014).
- [112] W. Liu and M. R. Hoffmann, *J. Chem. Theory Comput.* **12**, 1169 (2016).
- [113] A. Scemama, T. Applencourt, E. Giner, and M. Caffarel, *J. Comp. Chem.* **37**, 1866 (2016).
- [114] N. M. Tubman, J. Lee, T. Y. Takeshita, M. Head-Gordon, and K. B. Whaley, *J. Chem. Phys.* **145**, 044112 (2016).
- [115] Y. Garniron, A. Scemama, P.-F. Loos, and M. Caffarel, *J. Chem. Phys.* **147**, 034101 (2017).
- [116] M. Dash, S. Moroni, A. Scemama, and C. Filippi, *J. Chem. Theory Comput.* **14**, 4176 (2018).
- [117] Y. Garniron, A. Scemama, E. Giner, M. Caffarel, and P.-F. Loos, *J. Chem. Phys.* **149** (2018).
- [118] P.-F. Loos, A. Scemama, A. Blondel, Y. Garniron, M. Caffarel, and D. Jacquemin, *J. Chem. Theory Comput.* **14**, 43604379 (2018).
- [119] D. Hait, N. M. Tubman, D. S. Levine, K. B. Whaley, and M. Head-Gordon, *J. Chem. Theory Comput.* **xx**, xx (2019).
- [120] An alternative straightforward approach does not have a large memory requirement, but requires considerably larger computation time.
- [121] J. E. Smith, B. Mussard, A. A. Holmes, and S. Sharma, *J. Chem. Theory Comput.* **13**, 5468 (2017).
- [122] J. R. Trail and R. J. Needs, *The Journal of Chemical Physics* **139**, 014101 (2013).
- [123] J. R. Trail and R. J. Needs, *The Journal of Chemical Physics* **142**, 064110 (2015).
- [124] J. R. Trail and R. J. Needs, *The Journal of Chemical Physics* **146**, 204107 (2017).